Aeroacoustics of Space Vehicles

Jayanta Panda
NASA Ames Research Center
Moffett Field, CA

Presentation for

Stanford Fluid Mechanics Seminar

Jan 28, 2014

- **Aeroacoustics for Airplanes**
  - o Mostly for community noise reduction
  - o very few vibro-acoustics concerns (such as failures of nozzle cowlings)

- **Aeroacoustics for space vehicles**

o Mostly for vibro-acoustic concern

o Intense vibrational environment for payload, electronics and navigational equipment and a large number of subsystems

o Community noise - little concern until recent time

o Environment inside ISS– separate issue

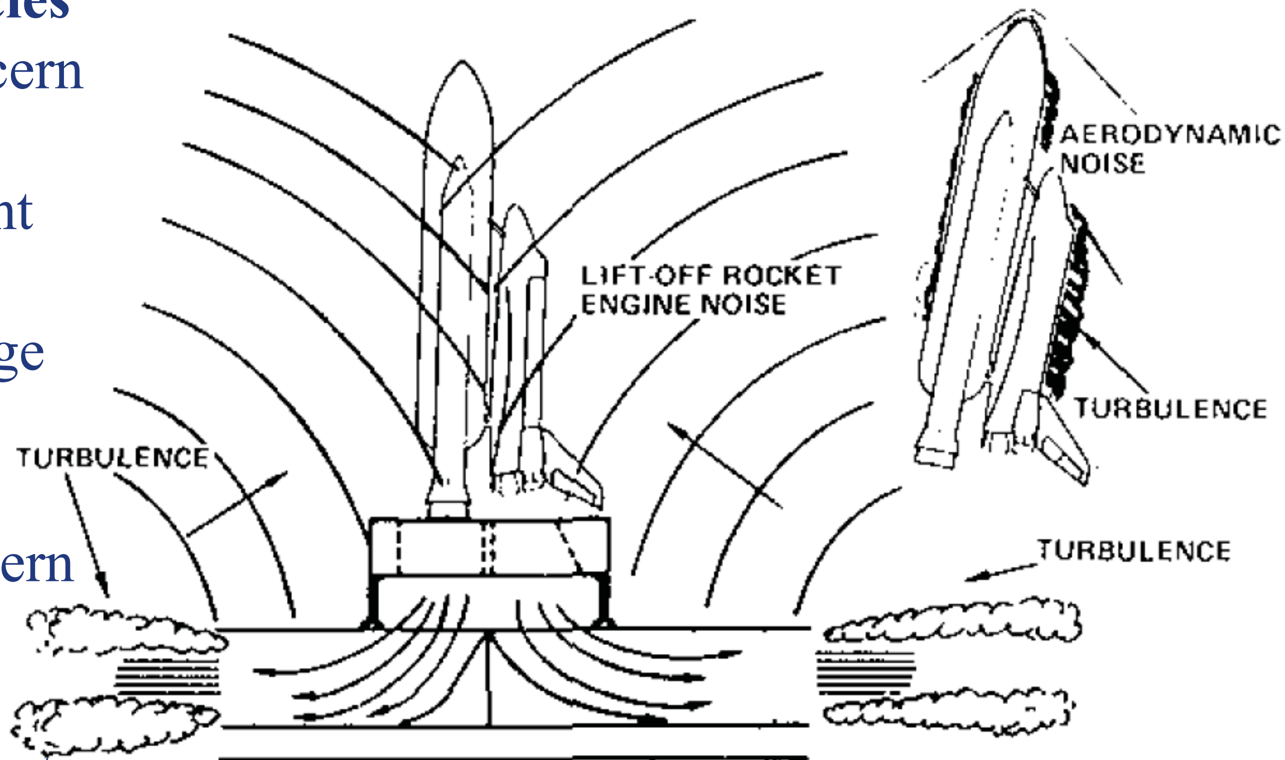

Fig. 1 Shuttle payload bay vibration and acoustic environment sources.

Typical levels (dB) of surface pressure fluctuations on launch vehicles

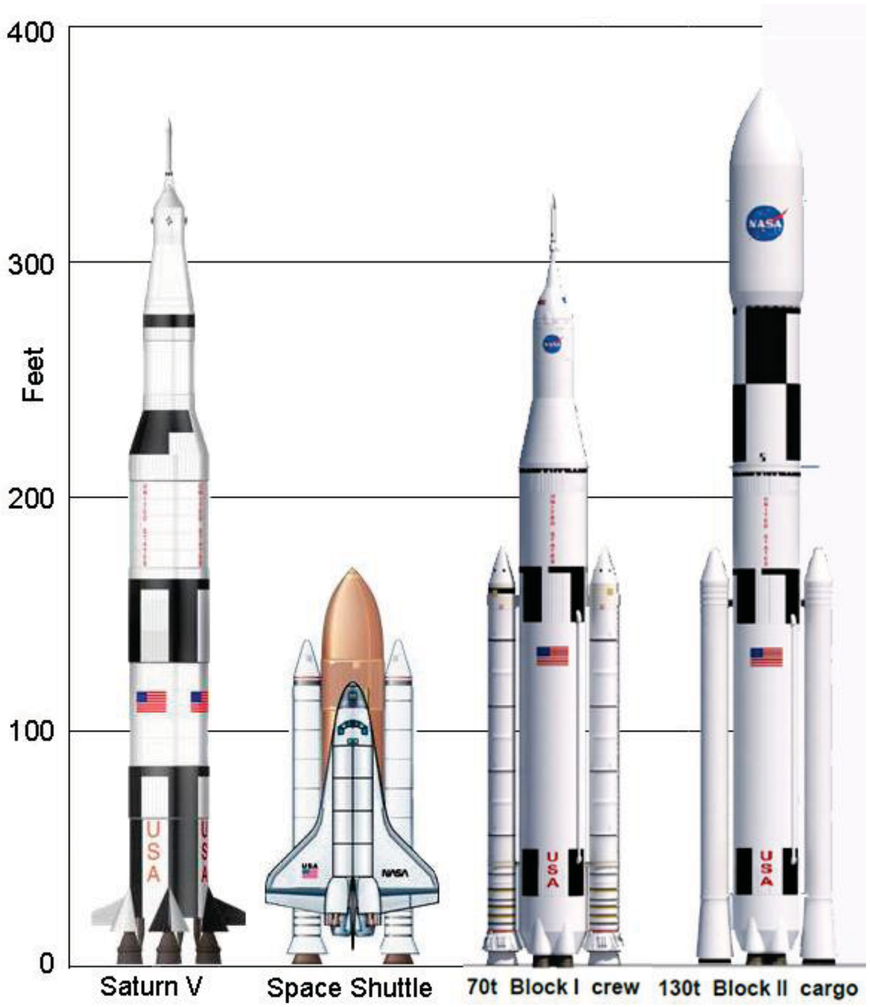

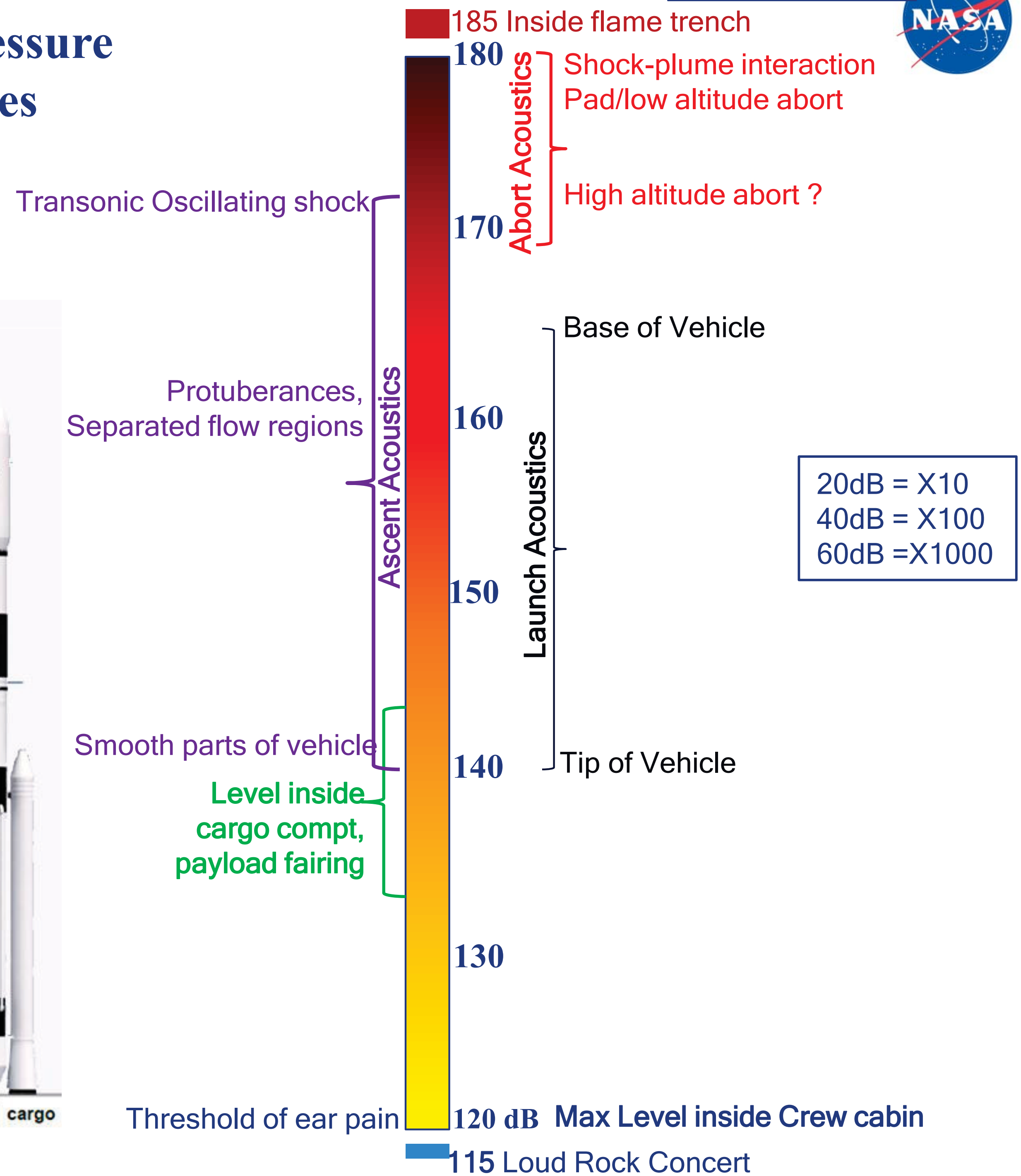

The end goal of acoustic analysis is to predict structural responses due to acoustic loads

3.1 Acoustic-Load Parameters

NASA SP-8072

To the extent required for design, the predicted acoustic loads shall be given as a function of position and time in terms of:

- Overall sound-pressure level
- Frequency spectrum
- Spatial correlation

2.2 Vehicle Loading

The minimum description of the loading on the vehicle, needed to estimate the structural response, is given in terms of the detailed distribution on the structure of the sound-pressure spectrum. A more detailed description also requires the spatial correlation pattern of the sound-pressure field to enable more exact vibration prediction. Such analyses are required for examining certain types of failures, such as the sonic fatigue of lightweight external panels.

Aeroacoustics : part of Fluids – Structure Interactions

NASA CR-1596: Himelblau, Fuller, Scharton, "Assessment of space vehicle aeroacoustic-vibration prediction & testing"

the displacement spectral density for location x at each frequency f due to a spatially-distributed applied loading is

$$G_w(x,f) = A^2 G_{pr}(f) \sum_{i=1}^{\infty} \sum_{k=1}^{\infty} \frac{\phi_i(x)\phi_k(x)H_i^*(f)H_k(f)j_{ik}^2(f)}{(2\pi)^4 f_i^2 f_k^2 M_i M_k} \qquad (2)$$

Structural response; area; Acoustic auto-spectrum; Mode shape; Freq response including damping; Modal mass

where the cross-joint acceptance function is given by

$$j_{ik}^2(f) = \left[A^2 G_{pr}(f)\right]^{-1} \iint_A G_p(\underline{\xi},\underline{\xi}',f)\phi_i(\underline{\xi})\phi_k(\underline{\xi}')d\underline{\xi}d\underline{\xi}' \qquad (2a)$$

Acoustic cross-spectrum

- Modelling via splitting the problem into aero-acoustics and vibro-acoustics

Separation of fluid dynamics and structural dynamics

- Aero-acoustics as a part of combined load

● **Forcing function** - Distribution of Auto and Cross-spectra of acoustic pressure fluctuations

Diffused Acoustic Field

$$G_{12} = \overline{G}_d(f)\frac{\sin(k_0 d)}{k_0 d}$$

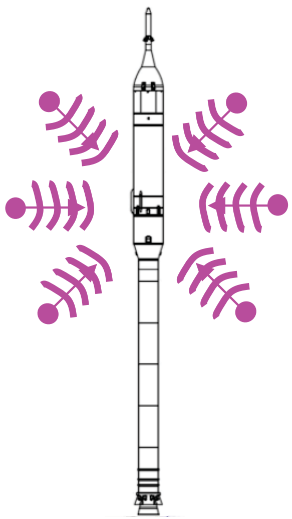

Progressive Wave Field

$$G_{12} = \overline{G}_p(f)e^{-c_d k_t d}\left[\cos(k_t d) - i\sin(k_t d)\right]$$

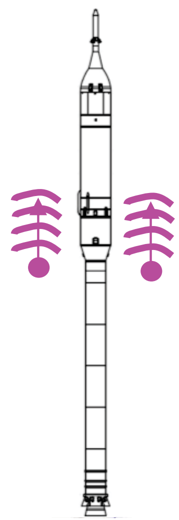

G_d = DAF autospectrum
G_p = PWF autospectrum

$k_t = \omega/U_t$ = trace wavenumber
$k_0 = \omega/c_0$ = acoustic wavenumber

d = separation distance
c_d = correlation decay coefficient

● **Prediction of Structural response** - forcing functions input to structural dynamics analyses - FEM, BEM, SEA models of the components, systems and subsystems of the vehicle.

Vibro-Acoustics tests for flight certification

Reverberant Acoustic Test Facility
NASA Plum Brook Station

One of the 25Hz horns in the test chamber

Mechanical Vibration Facility

Roadmap:

- Launch Acoustics
  - o Description of launch pad
  - o Prediction, CAA
  - o Static fire test
  - o Flight test
  - o Identification of acoustic sources During Antares launch by a microphone phased array
- Ascent Acoustics
- Abort Acoustics

Why study launch acoustics?

- Very high acoustic level during launch creates high vibro-acoustics environment
  - ► All payloads, many parts of the vehicle, and ground op systems need to be designed, tested and qualified for this environment
  - ► The fluctuation levels influence the weight and the cost of the vehicle

- The acoustic suppression systems needs to perform optimally to provide relief

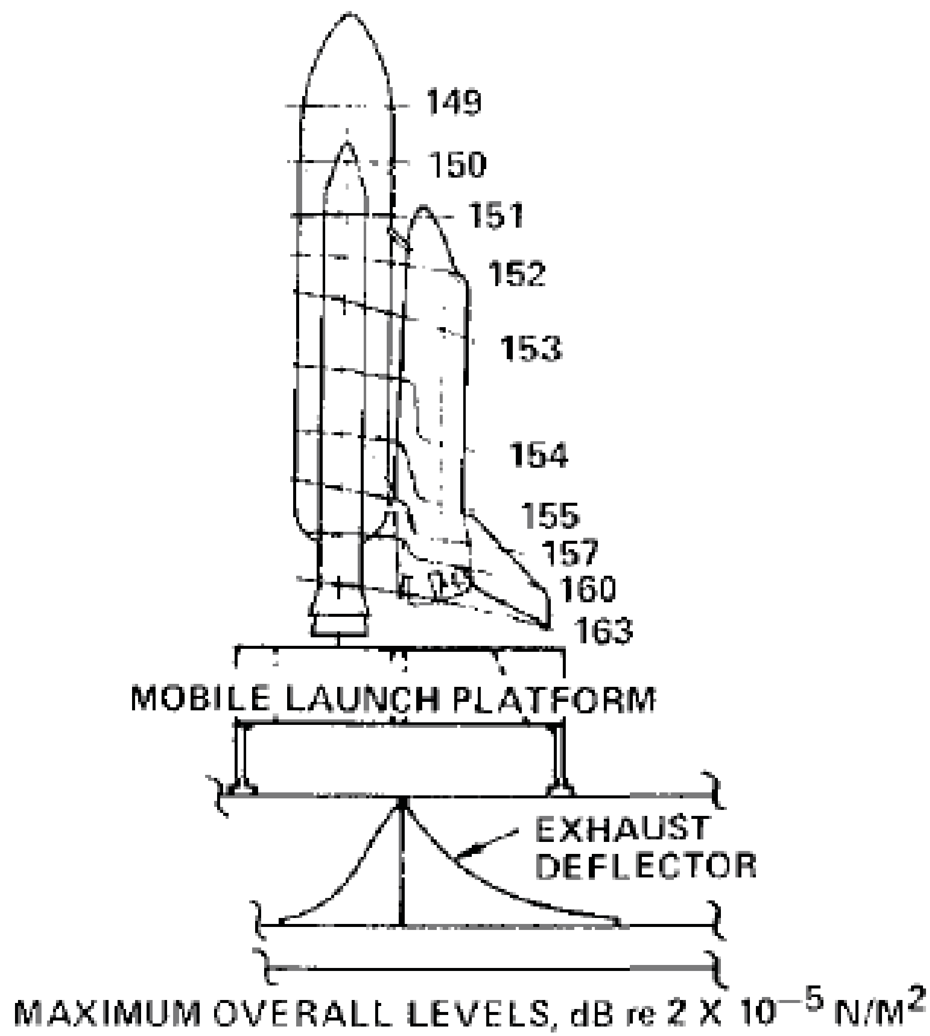

Fig. 2 Engine noise levels during Shuttle lift-off.

Launch pad design and acoustic suppression system

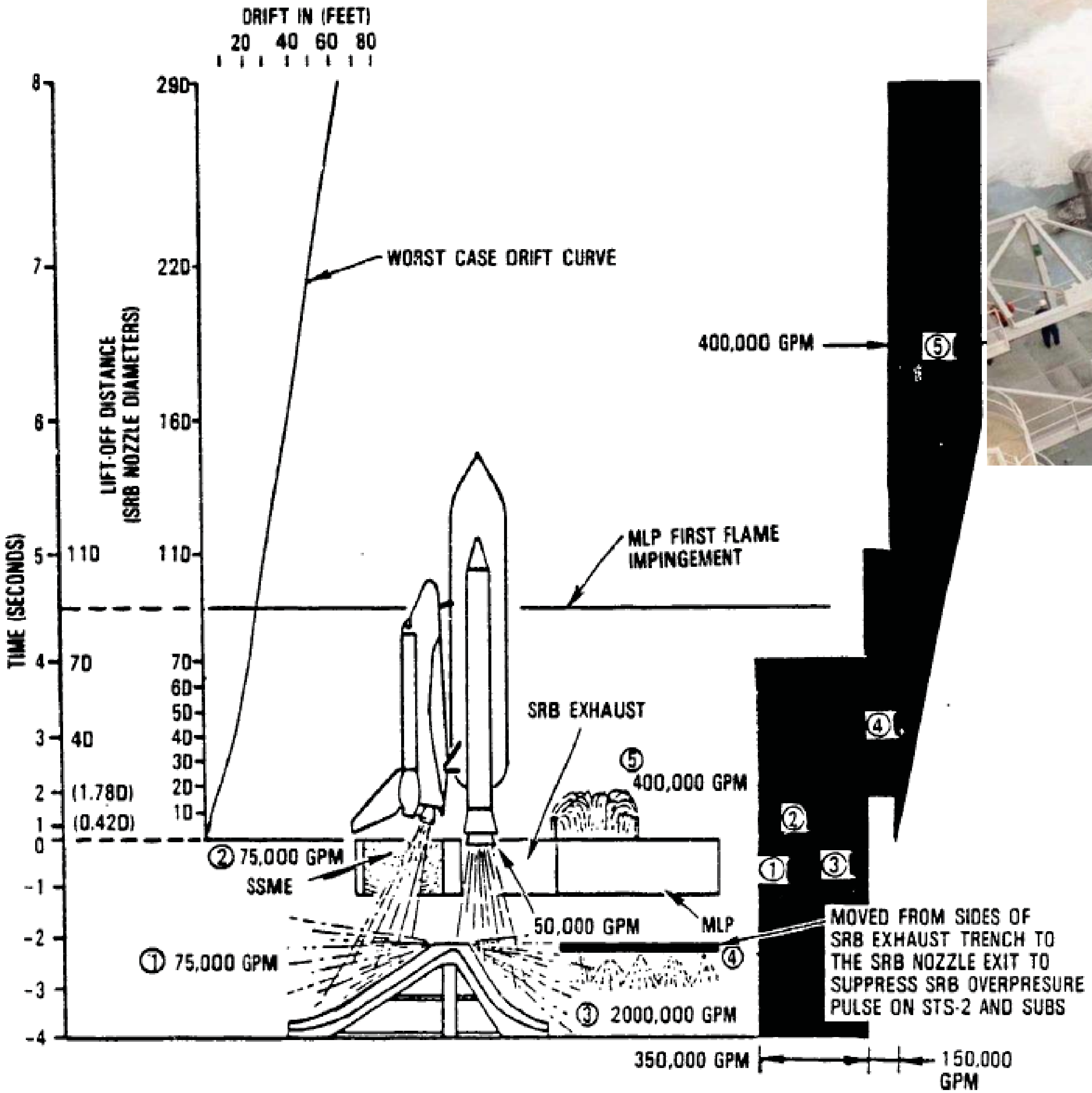

Shuttle Pad water injection

- Deflector
- Trench/Duct
- Mobile launch platform
- Service Tower
- Water flow systems
- Vehicle trajectory
  - elevation
  - drift

Prediction – NASA SP-8072, "Rocket Vehicle Liftoff Acoustics and Skin Vibration Acoustic Loads Generated by the Propulsion System" **1971**

- There exists no prediction methodology from the fundamental equations
- Total acoustic power W_a is related to the mechanical power W_m generated by the rocket, η = efficiency factor 0.2% to 0.8%

$$W_a = \eta W_m = \eta \sum_{All\ nozzles} 0.5(Thrust)\,U_{exit}$$

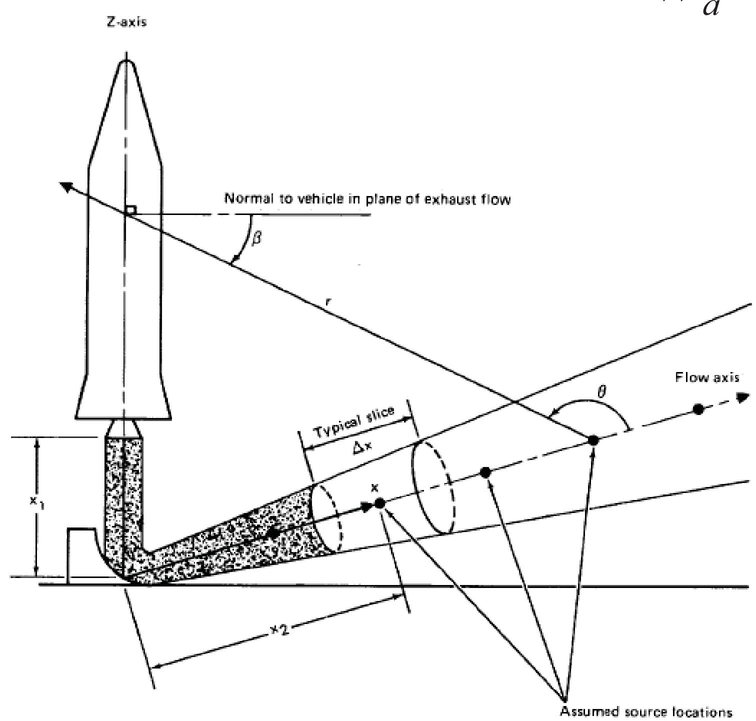

Distributed source along plume path

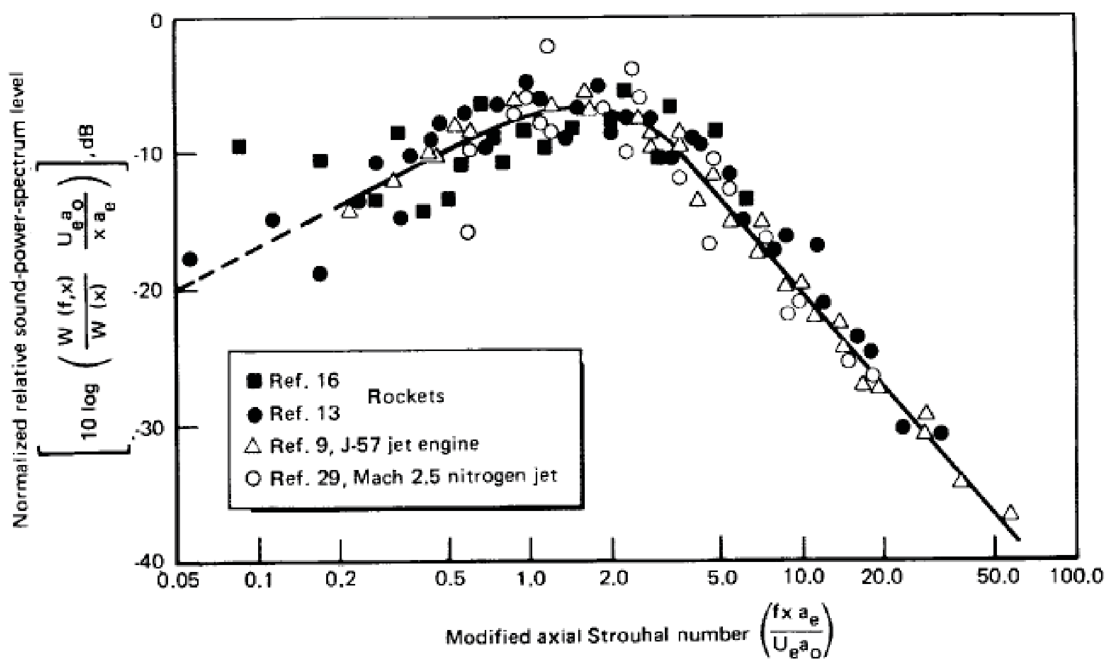

Figure 13. – Normalized relative power-spectrum level as a function of axial position along the flow for chemical rockets and jets.

Prediction - based on flight data from prior vehicles

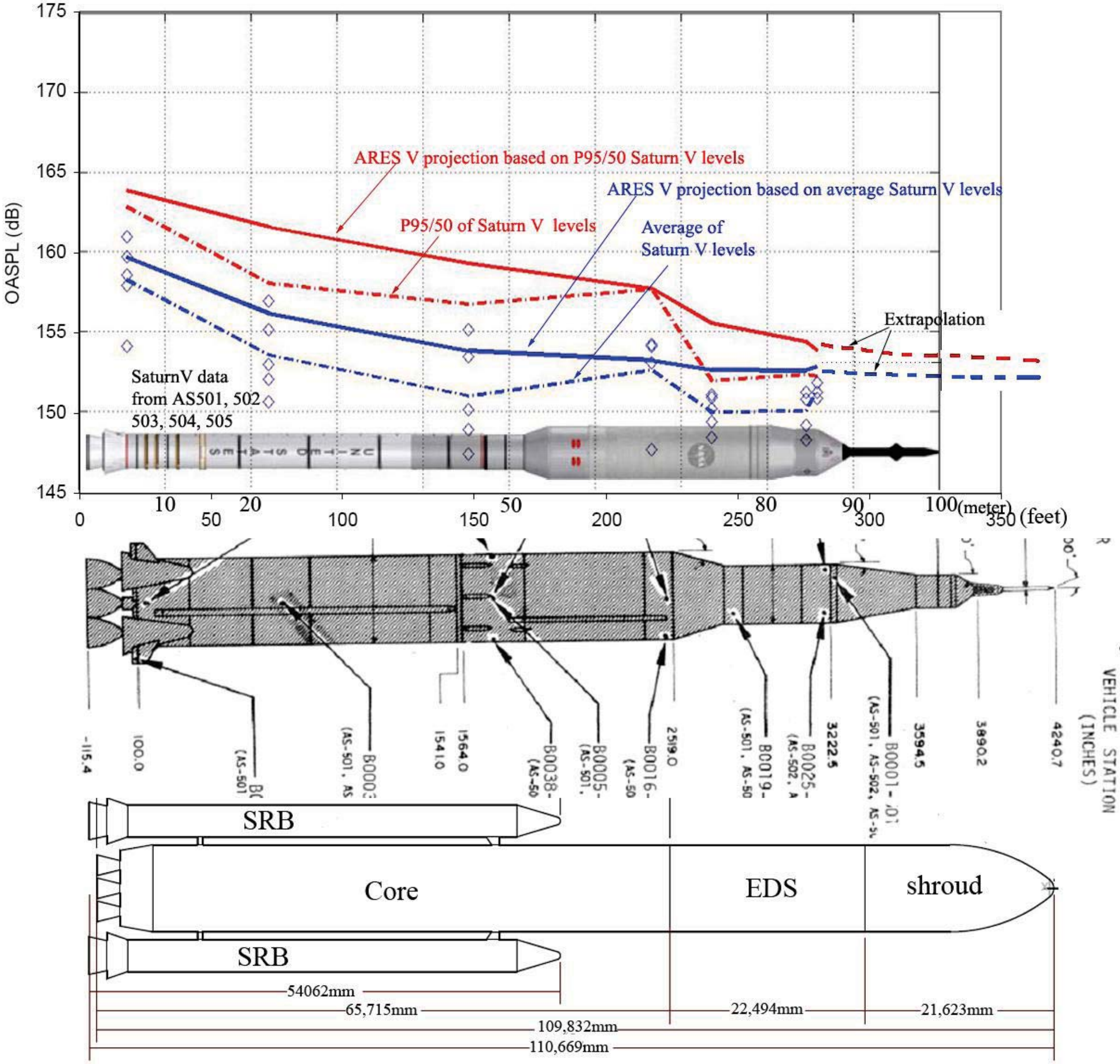

Acoustic data books

- Apollo – Saturn
- Space Shuttle
- Ares-IX

- Scaling based on engine thrust, and Strouhal frequency.

Prediction - CAA

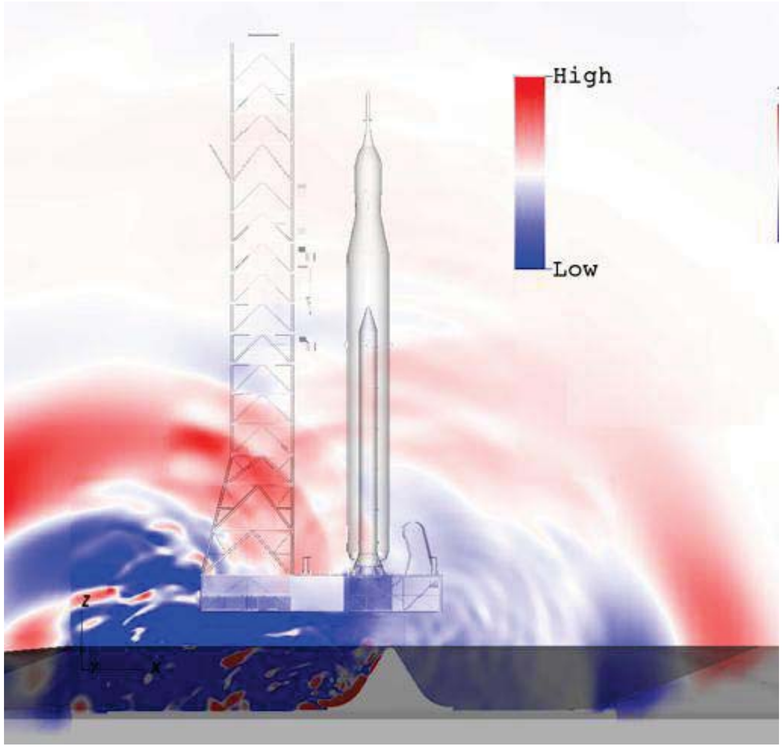

SLA Launch simulation, NASA Ames
LAVA code, Kiris et al, AIAA 2014-0070.

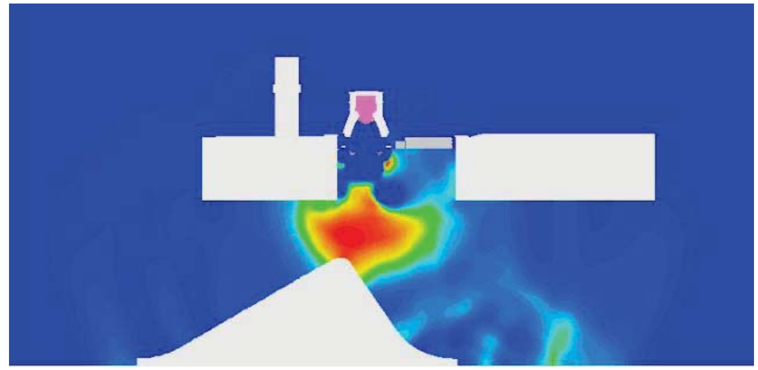

Pressure pulse after Ignition, J. West, MSFC

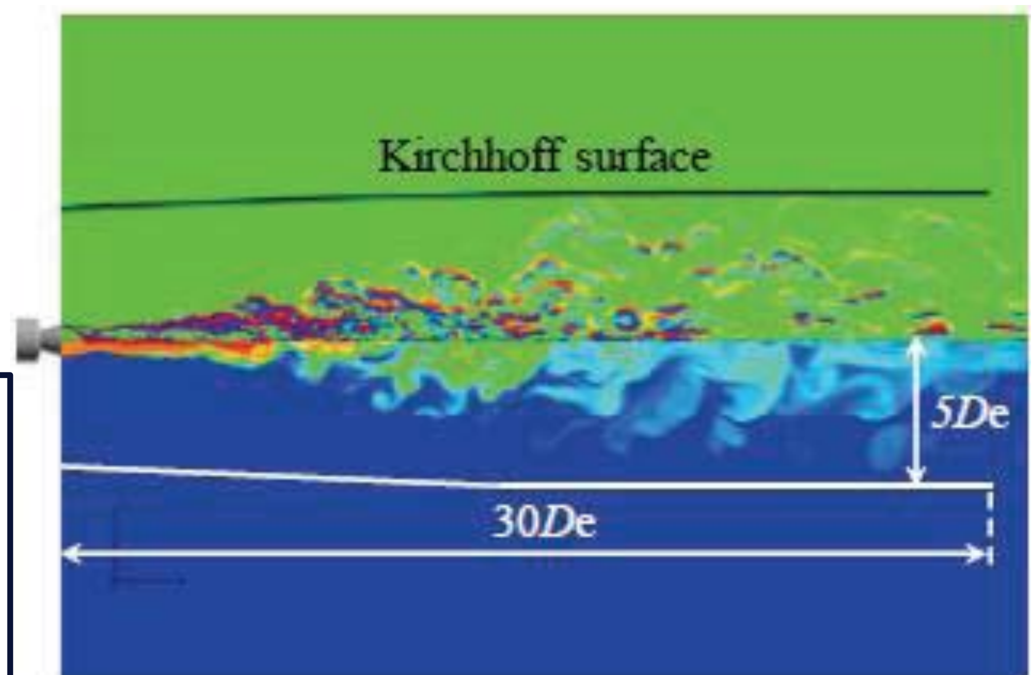

LES simulation: Fukuda et al, 2009
Effect of water injection: Fukuda et al, 2011

Challenges –
⇒Complex geometry, high Re, multi-phase flow, multiple γ, multiple species

Paths for CAA simulation:
- RANS + acoustic analogy
- LES
- Need of experimental data for validation

Model scale static fire tests - ASMAT

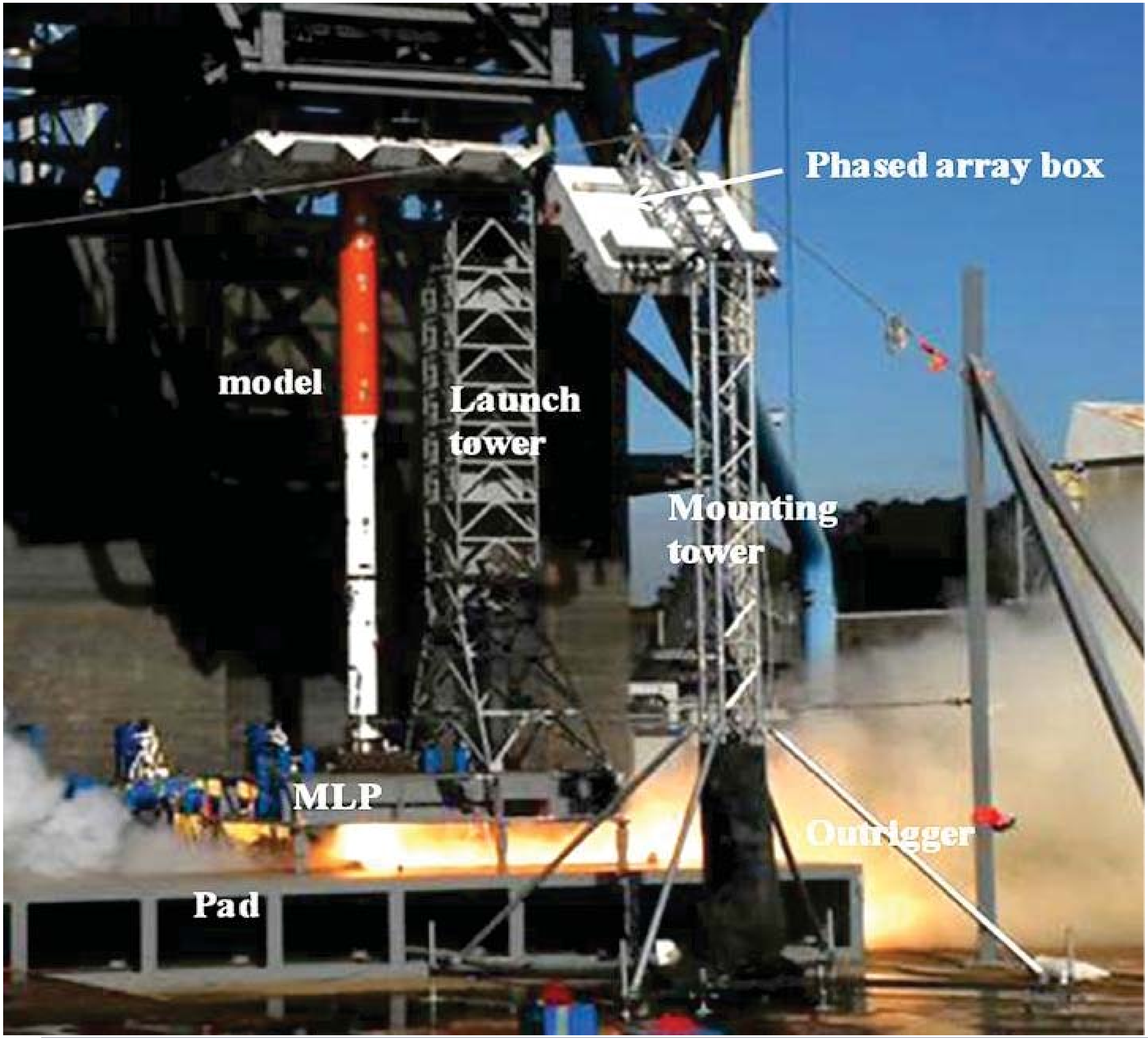

Static fire tests are the best means to determine

- launch environment
- water schedule
- pad modification

- 5% scale model of **ARES I**

Validation/adjustment from Flight sensors

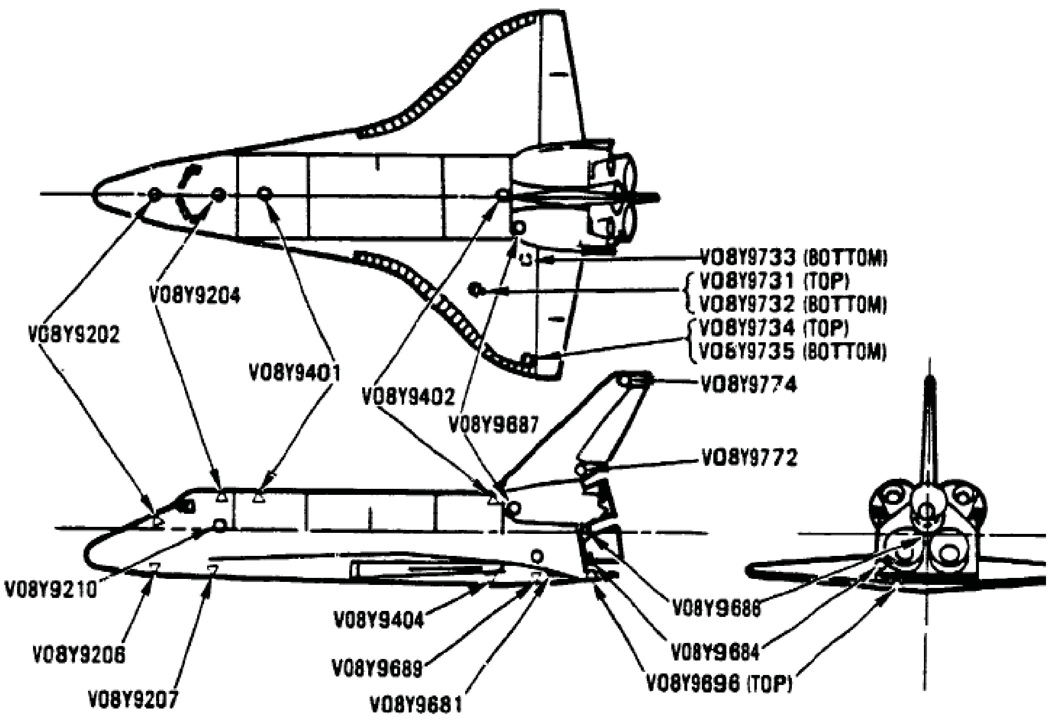

External **microphones** on Orbiter

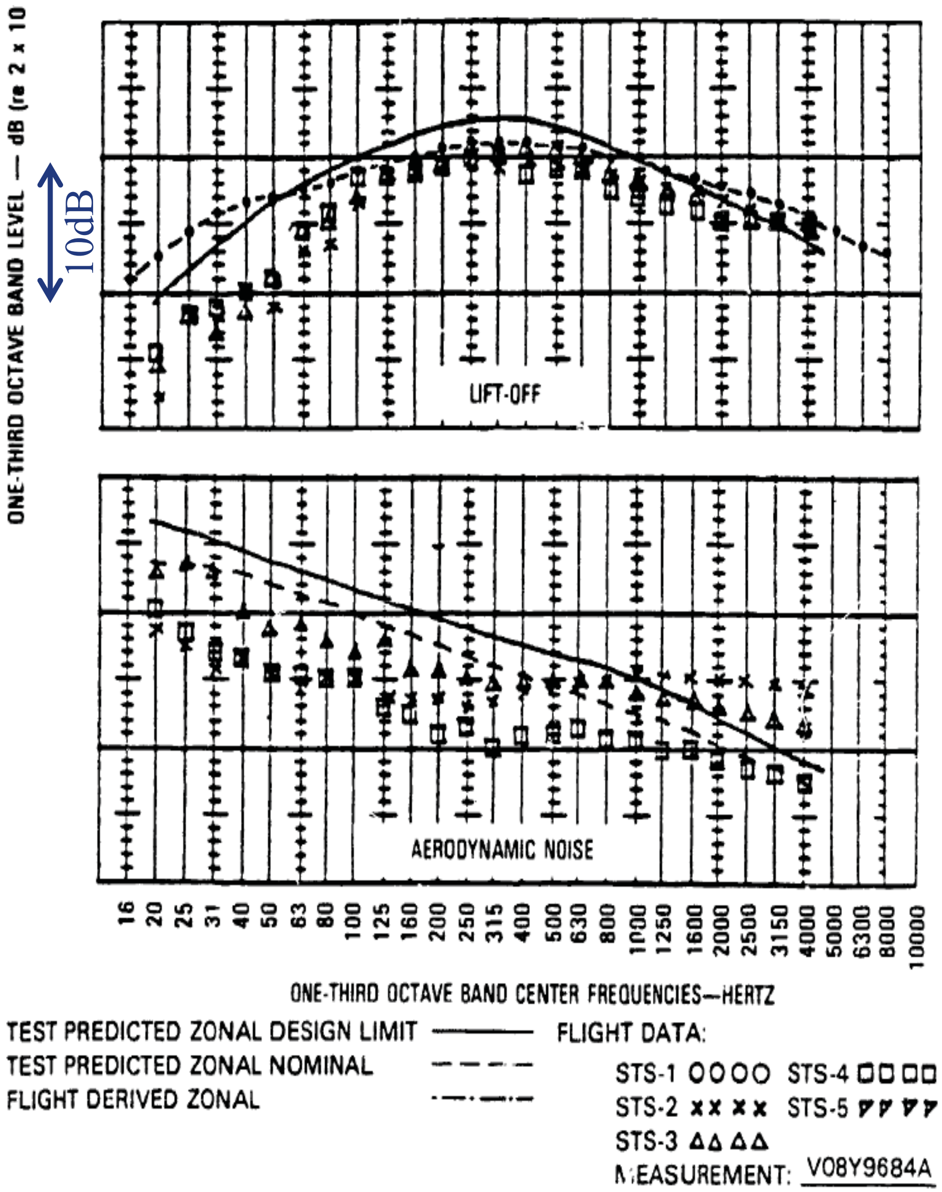

What are the true sources of noise during liftoff? - Use of microphone phased array

- Phased array – Acoustic camera, a tuned ear.
- Ubiquitous in Aeronautics, new in Space applications
- Need for a large size array for a full-scale vehicle application

→ ***Angular resolution of array ~ (acoustic wavelength) / (array aperture)***

- Design of a brand new array
  - ►10'X10' size, use 70 microphones
  - ► lighter weight
  - ► weather protection
  - ► debris protection
  - ► vibration isolation for camera

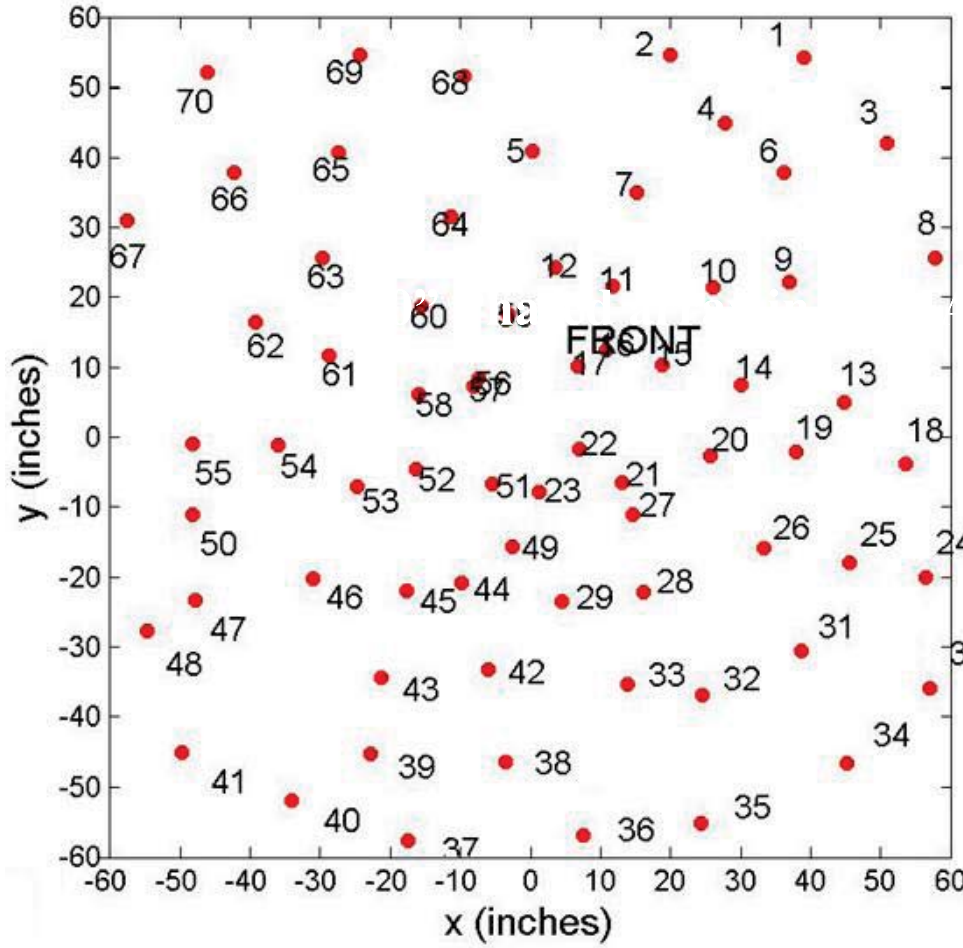

Microphone pattern for new 10' array

Evolution of phased array project

- Array validation in **Ames hybrid motor test**
  - ► revealed the need for solid state electronics
  - ► vibration isolation
  - ► need for rain protection

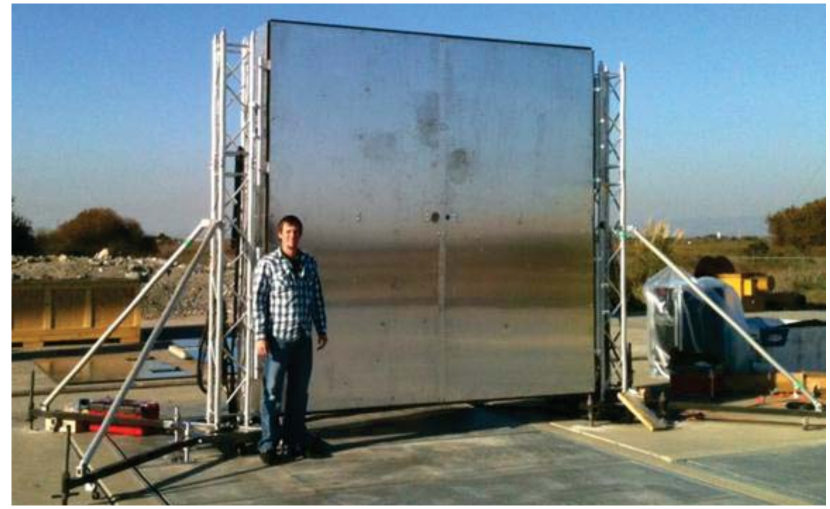

- Software
  - ► Conventional beamform

$$b_{jj}(f) = w_{j,m}{}^{\dagger} G_{m,m'}\, w_{j,m'}$$

  - ► Spectral Element Technique (SEM) provided most promise

$$E(\alpha_j, f) = \sum_{m,m'=1}^{J} \left| G_{mm'} - \sum_{j=1}^{N} w_{j,m} \alpha_j^2 w_{j,m'}^{*} \right|^2$$

- All **hardware shipped to NASA Wallops**

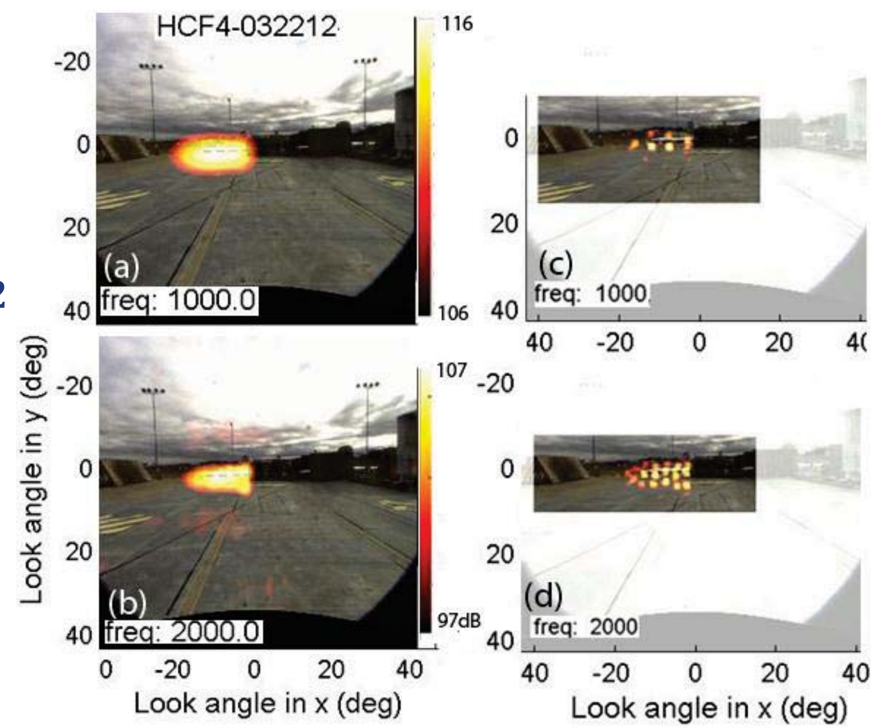

Noise map during hybrid motor burn

Phased array set-up at Wallops pad 0A

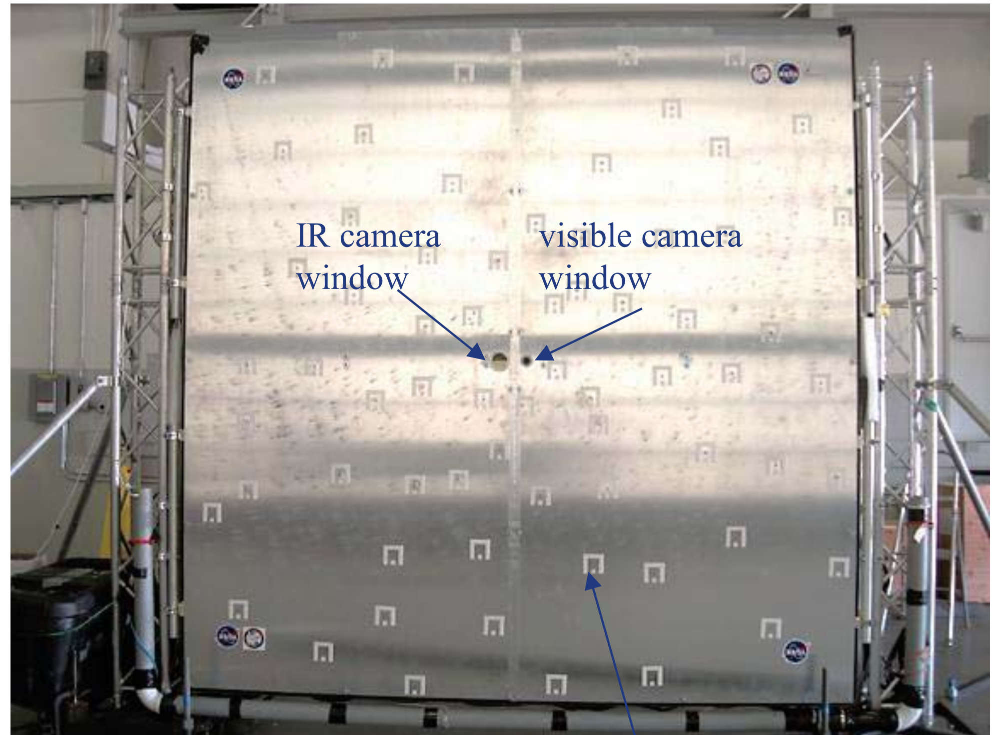

(front view) **Mylar cover for each microphone**

Instrumentations:

- 70 condenser microphones
- 1 visible band camera
- 1 long wave Infra-red camera
- 1 x-y accelerometer

The phased was mounted on a scissor lift at south side of pad 0A, ~ 400' from the Antares Engine, & 40' above ground

Phased array in Antares A-one launch: April 21, 2013

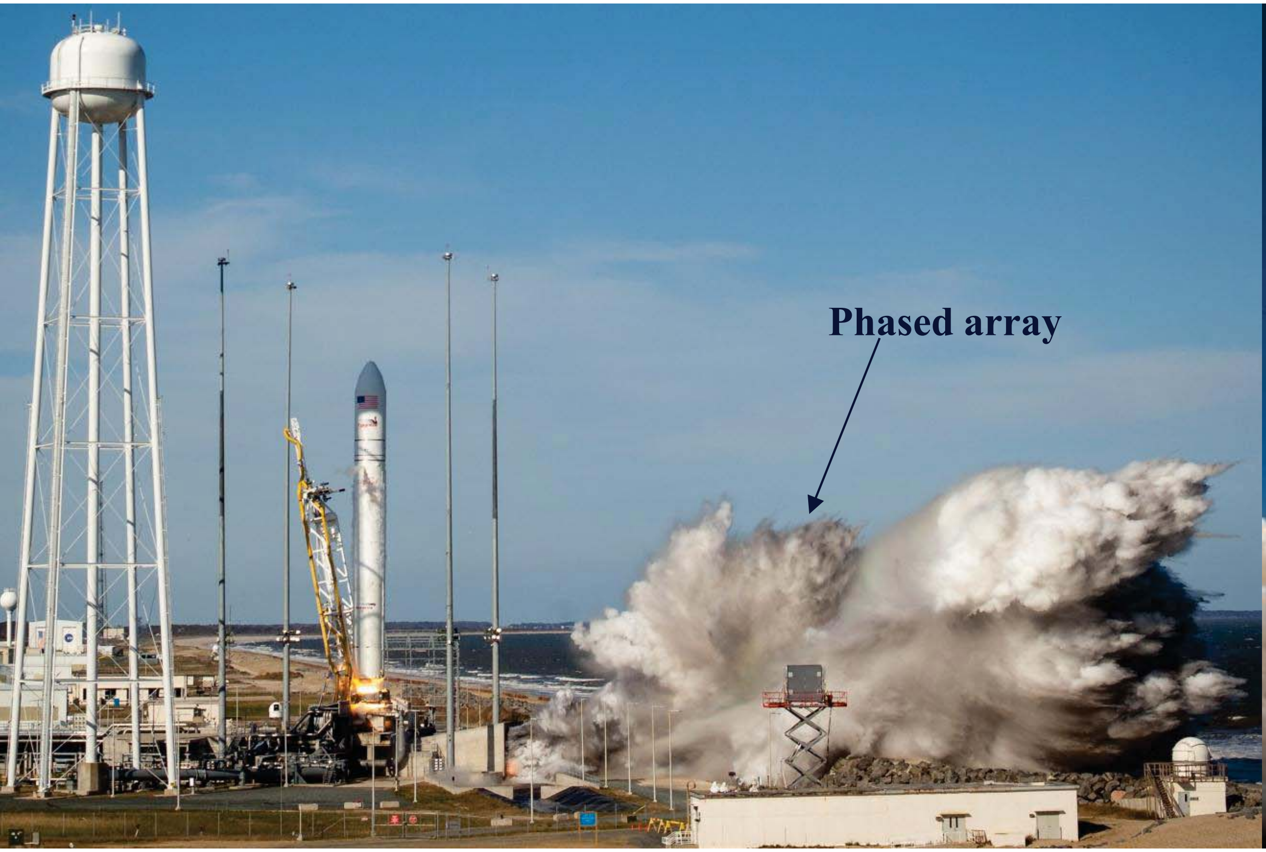

Rest of the presentation is from A-one launch

Acoustic Attenuation Systems

◀Water injection inside launch mount (on the top of the flame trench).

On-deck water injection using 4 Rain-bird heads ▶

- Water started to flow from 3 short rainbirds at t+5.7s
- Water started to flow from 1 tall rainbird at t+6.8s
- Tall rainbird is 6' taller than rest
- It takes ~2s to build full flow.

Initial Trajectory

- Slow moving vehicle
- TEL avoidance maneuver to avoid contact with the service tower

Time dependent beam-forming:

- Microphone time signals were segmented into 0.2s wide segments

Propagation delay:

- Microphones received the launch events at a delayed time. ~ 0.4s for sounds to propagate from the launch pad to the phased array.

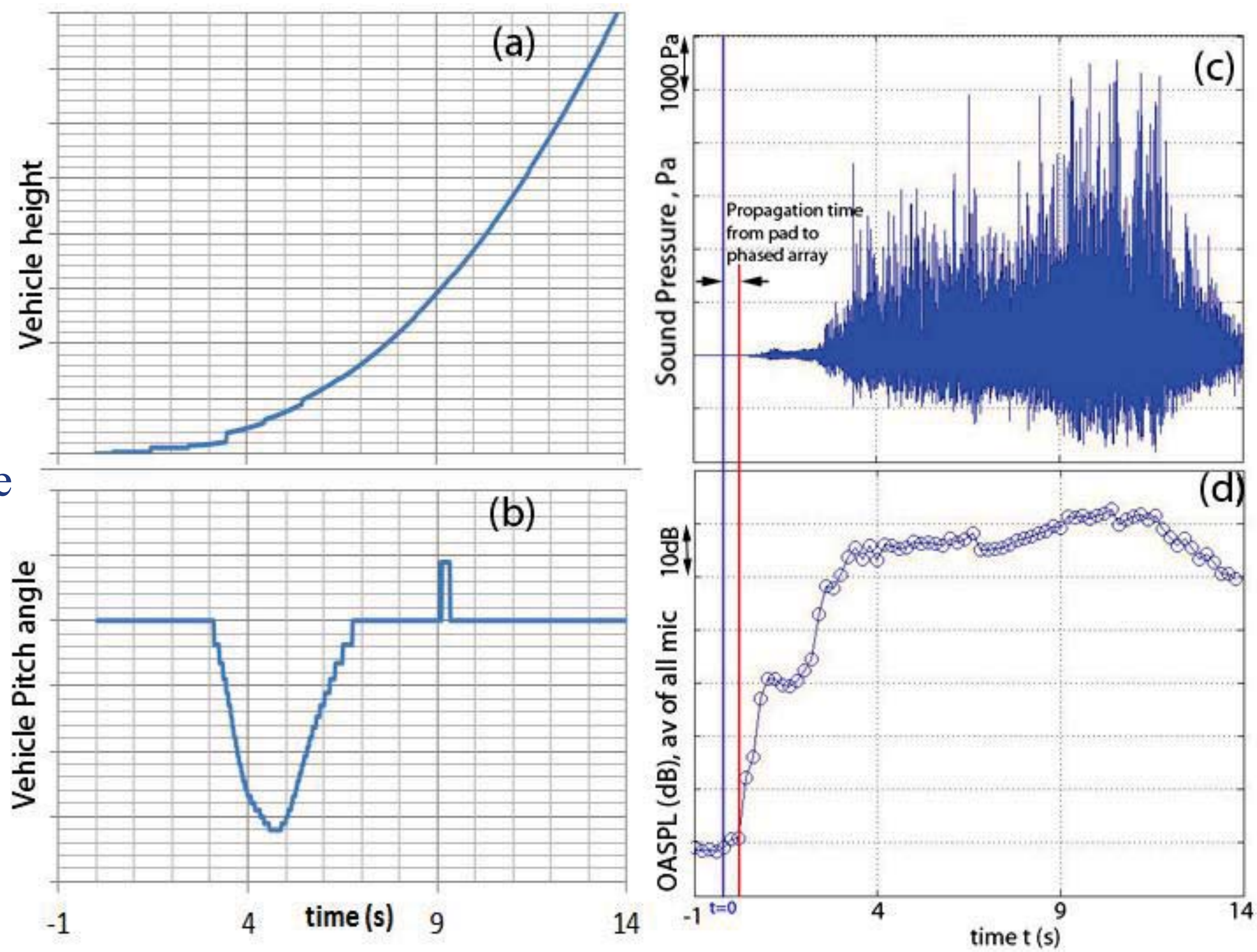

Noise source map at t+0.6s, conventional beam-form at 2kHz

Source strength at 2kHz in 80Hz wide band - ***Auto-scaled***

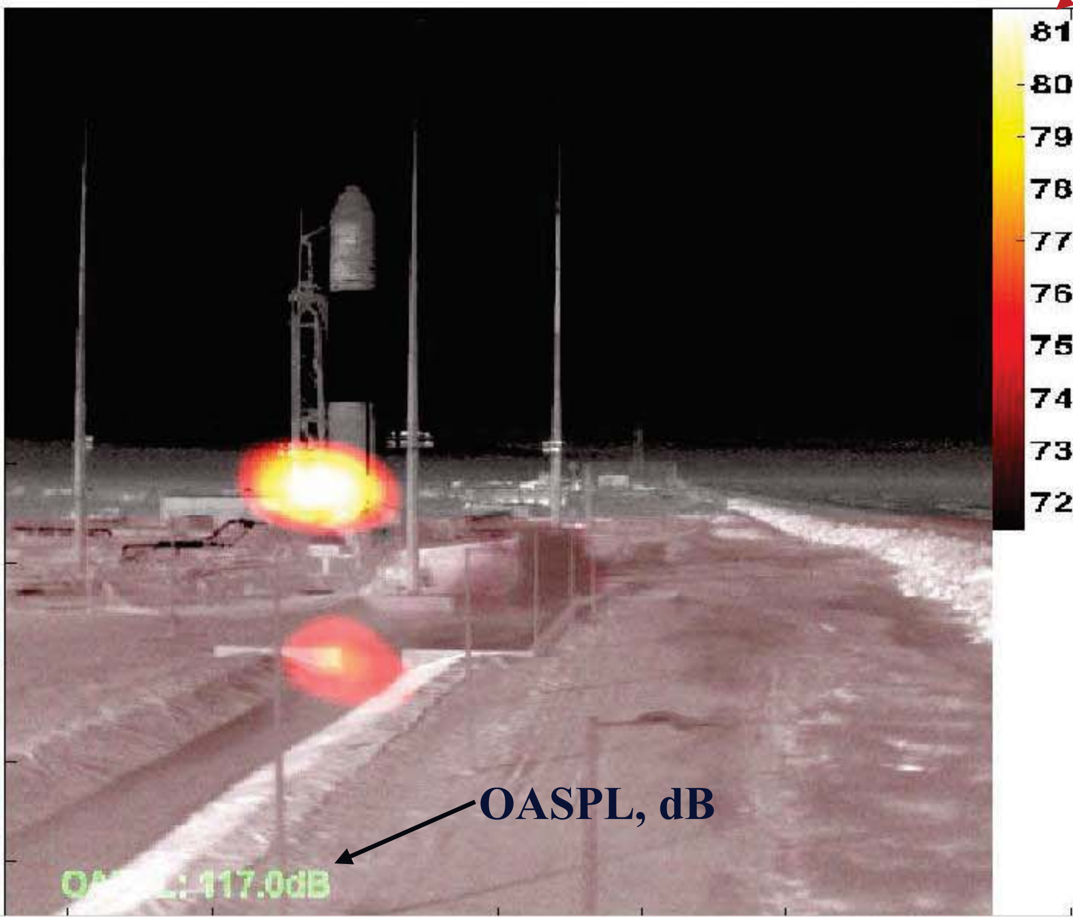

OASPL, dB

- Engine Ignition created noise source at launch mount
- Phased array, mounted 40’ above ground, saw both the primary source and its image on ground

Noise source map at t+2.9s

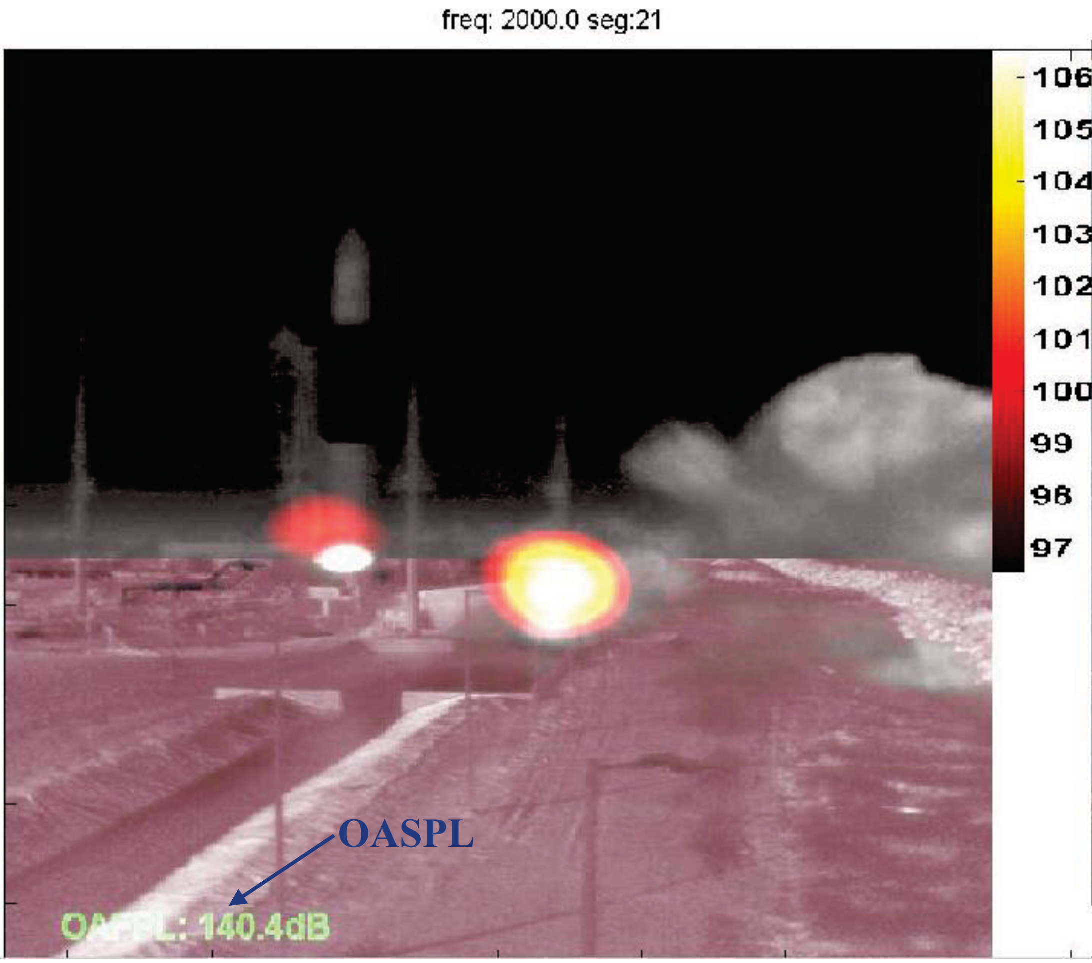

- The duct (trench) exhaust became the primary noise source as the hot plume started to come out (see movie).
- Effective cooling by duct water minimized the extent of the noise source
  – the OASPL was somewhat reasonable.
- Launch mount remained as a strong noise source.

Noise source map at t+5.7s

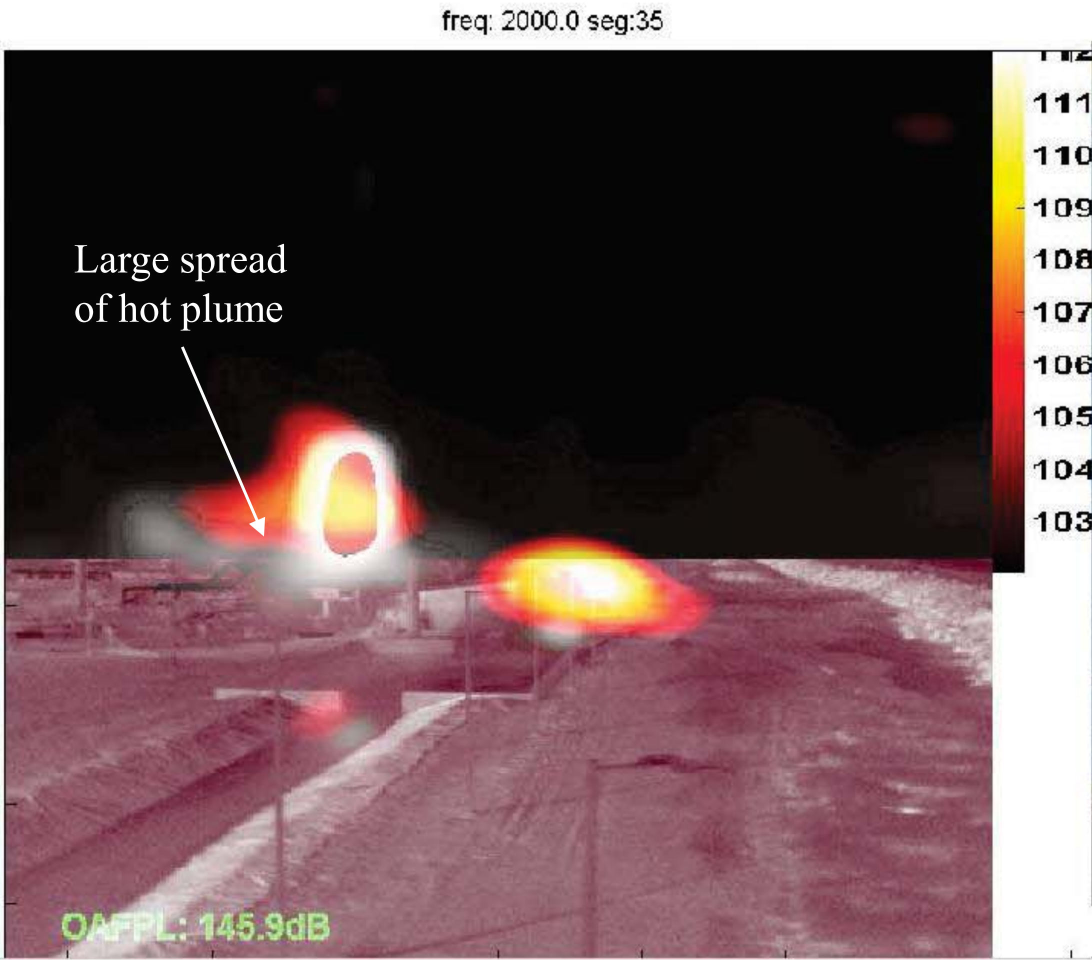

- Vehicle drifted even more towards east, caused heavy spreading of the hot plume over the pad, - Extended the size of the noise source.
- Start of flow from short 3 Rainbirds (not much water). No flow from 1 tall rainbird. Duct water in full force.

Noise source map at t+8.7s

- The long, exposed plume was the primary noise source.
- Still some impingement on the pad, yet the rainbird system had come to full force, and quenched the hot plume and the deck.
- From this time on, as the vehicle gained altitude and speed, the acoustic level on the vehicle was expected lower; however, ground service equipment did not see any decrease for another few seconds
- ground reflection

Optimization of Antares Water injection schedule

Hi Jay,
Yes the activation timing of the water deluge rainbirds was moved up from T+5s to T+3.8s.

Subject: Re: Antares Test Launch

Understood, thanks. Yes from a ground system standpoint, we also noted less ablative wear on the launch mount this time around, which is most likely attributable to faster water deluge activation. The phased array effort was indeed beneficial.

Ascent Acoustics

- o Vehicle trajectory and dynamic pressure
- o Buffet and acoustics
- o Prediction – empiricism and existing database, CFD
- o Wind tunnel tests
- o shape modification
- o Flight tests

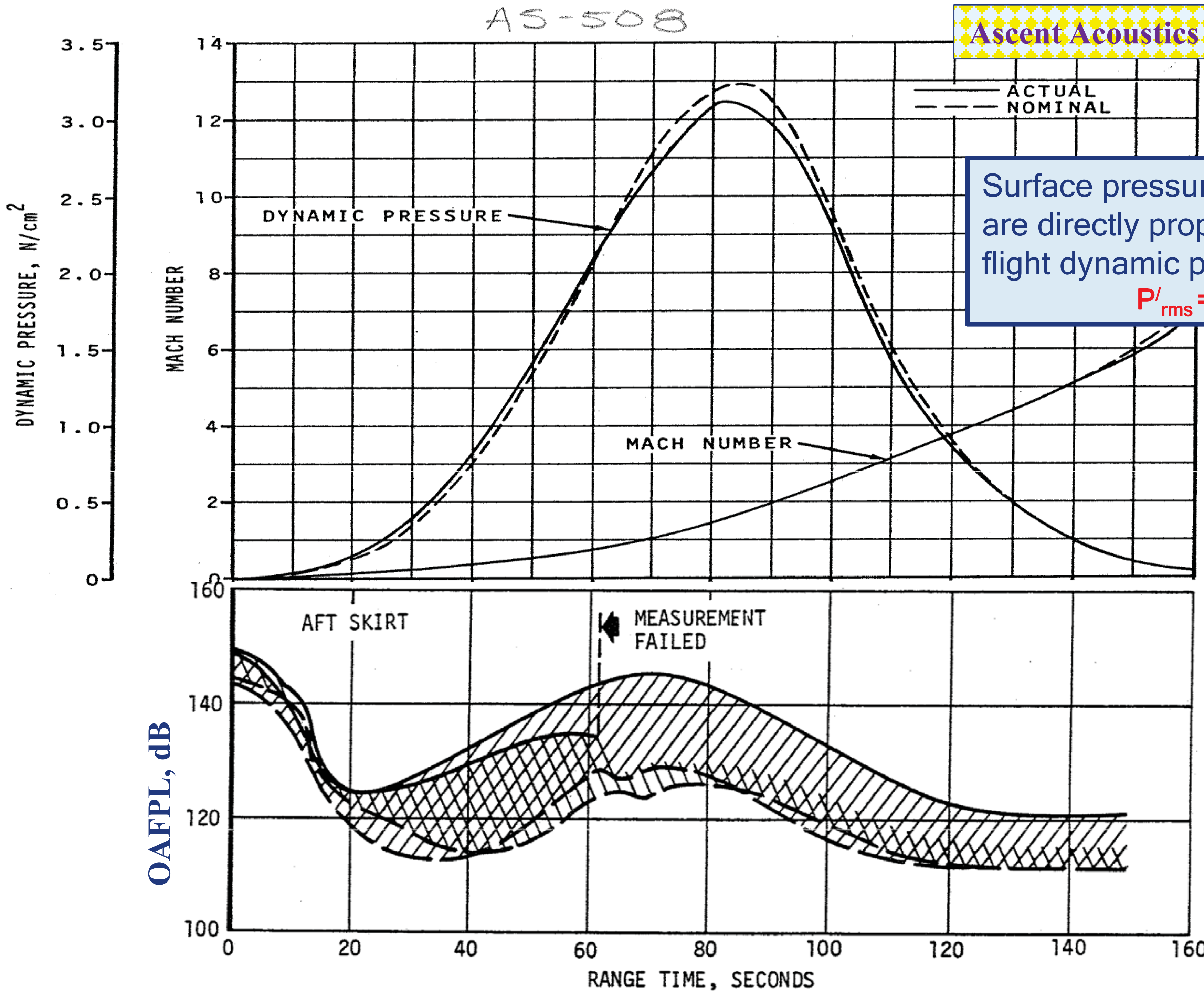

Surface pressure fluctuations are directly proportional to the flight dynamic pressure:

$P'_{rms} = k\,q$

Figure 16-16. S-IVB Acoustic Levels During S-IC Burn

Prediction - Aerodynamics of Launch Vehicle

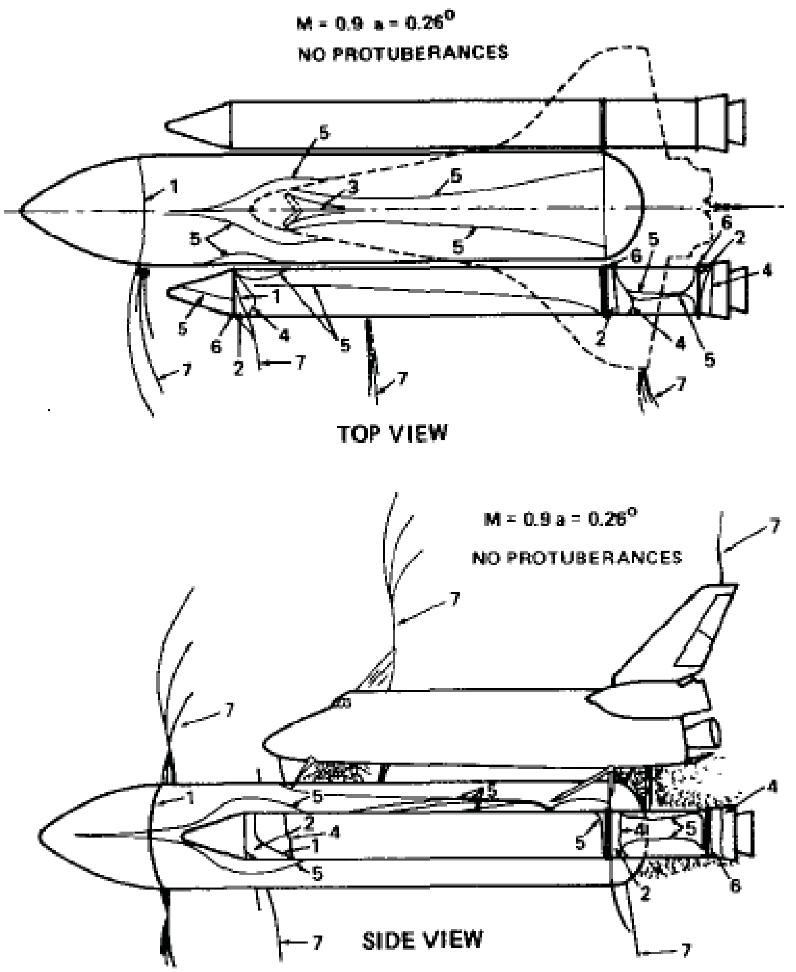

1 SHOCK LINE (OIL FLOW)
2 SEPARATED FLOW AREA
4 FLOW REATTACHMENT LINE
5 FLOW STREAMLINE
6 SEPARATED FLOW LINE
7 SHOCK (SHADOW GRAPHS)

NOTE: SKETCHED FLOW AT ET BASE REGION AND AFT OF FORWARD STRUT REPRESENTS A SEPARATED WAKE.

Fig 16 Shuttle aerodynamic flow field – Mach 0.9

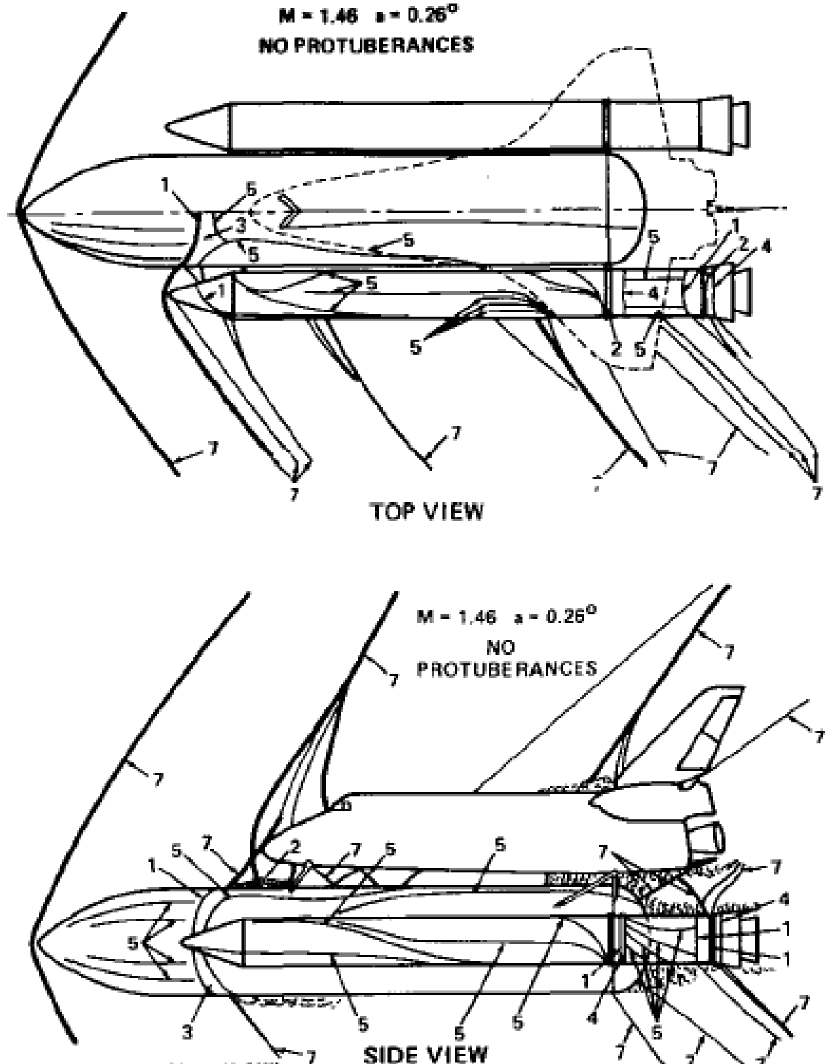

1 SHOCK LINE (OIL FLOW)
2 SEPARATED FLOW AREA
3 AREA OF UNDETERMINED FLOW
4 FLOW REATTACHMENT LINE
5 FLOW STREAMLINE
6 SEPARATED FLOW LINE
7 SHOCK (SHADOW GRAPHS)

NOTE: SKETCHED FLOW AT ET BASE REGION AND AFT OF FORWARD STRUT REPRESENTS A SEPARATED WAKE. FLOW ON ET LOWER SURFACE AFT OF SHOCK IS A TURBULENT BOUNDARY LAYER.

Fig 17 Shuttle aerodynamic flow field - Mach 1.46

Prediction - steady state CFD to determine input parameters for empirical relations

Attached turbulent boundary layer:

$$p_{rms} = q\frac{0.01}{1+M^2}$$

$$G(f) = \frac{4C\delta^* F^{1.433}}{U\left(!+C^2F^{2.867}\left(\frac{2\pi f\delta^*}{U}\right)^2\right)} p_{rms}^2$$

Use CFD database to determine boundary layer Displacement thickness δ*

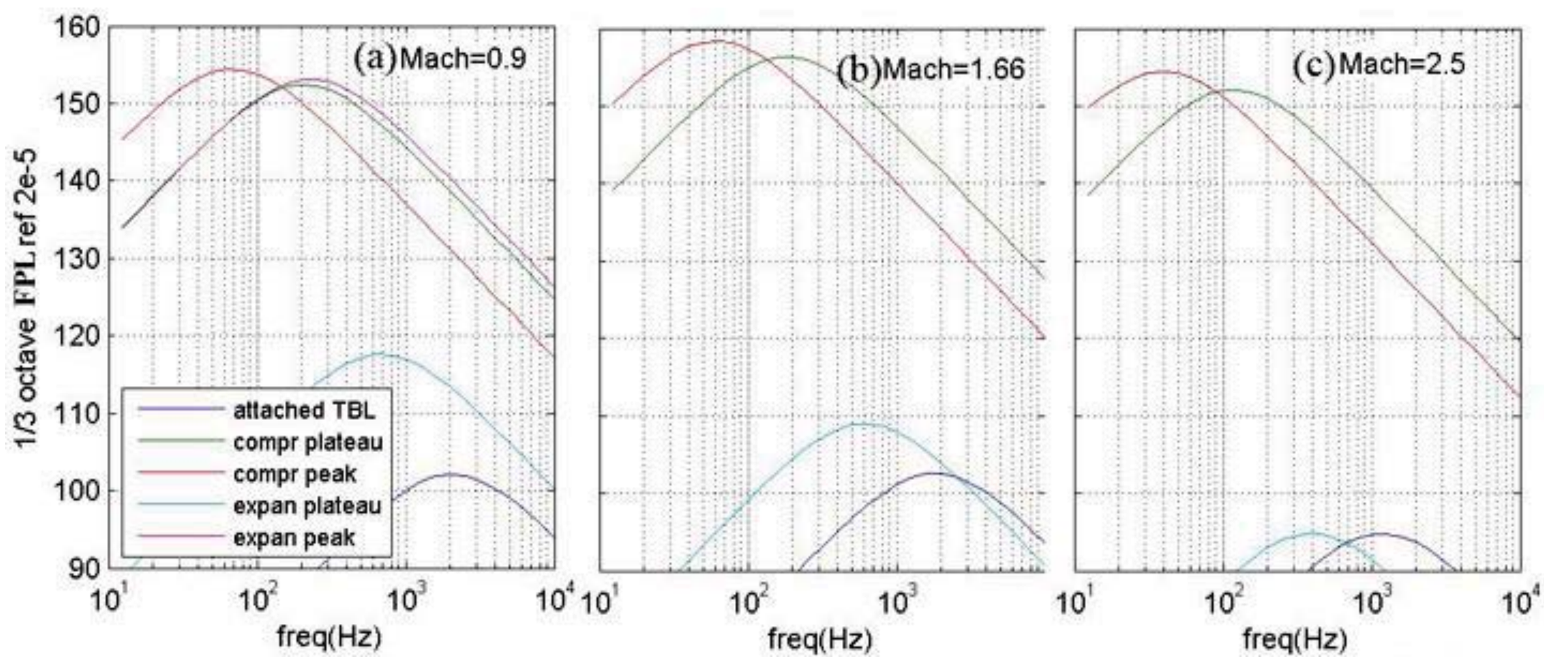

Calculated auto-spectra using empirical relations

Prediction - steady state CFD to determine input parameters for empirical relations

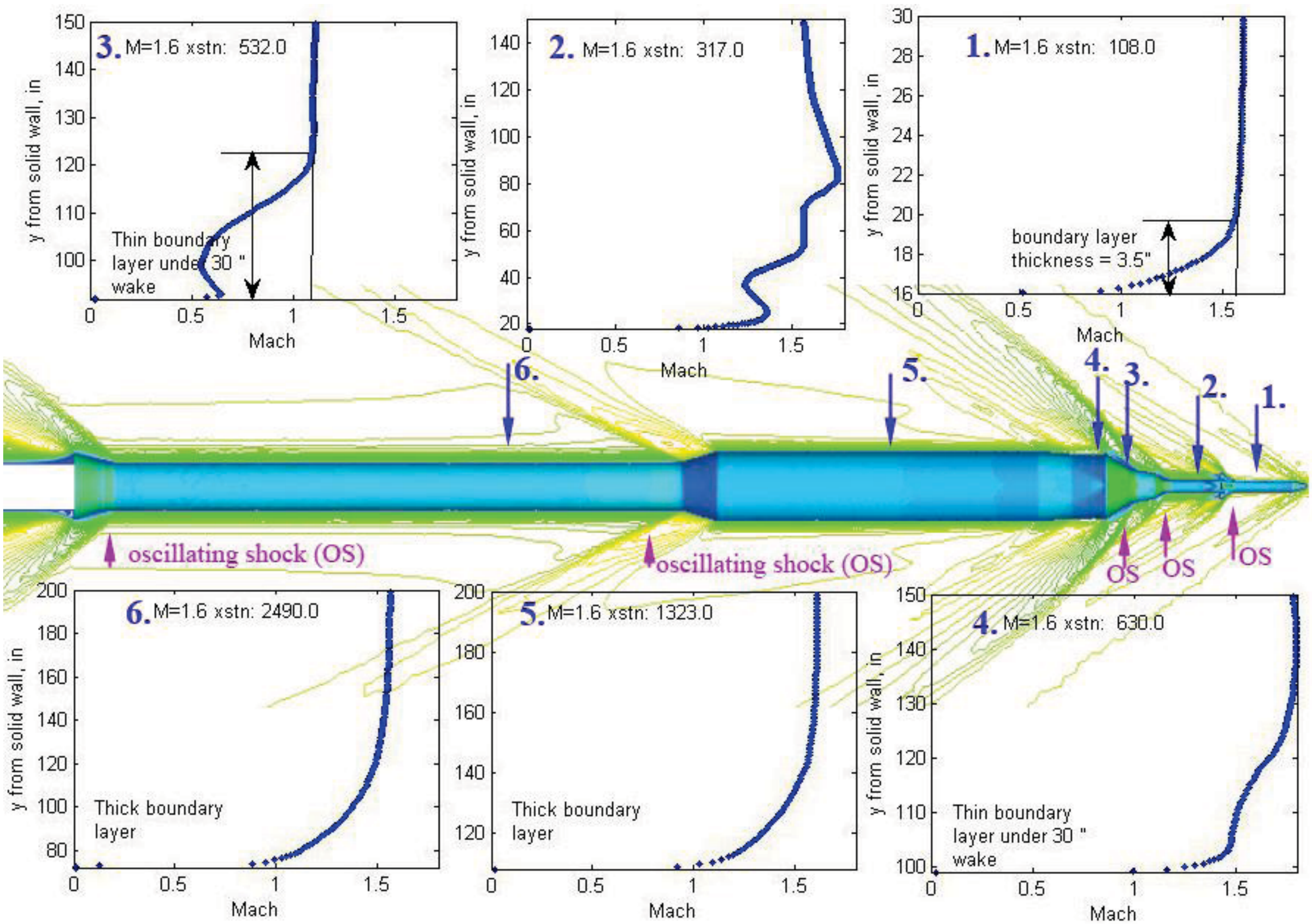

USM3D calculated flow-field over ARES IX at flight M = 1.6 (Source: Steve Bauer LaRC)

Prediction - based on flight data from prior vehicles

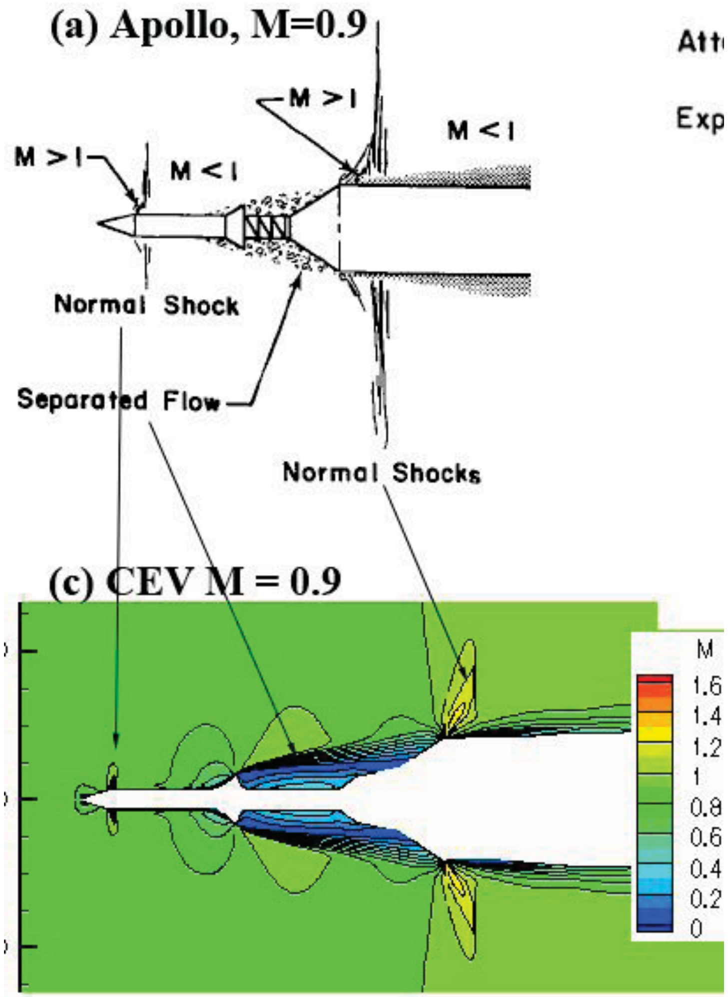

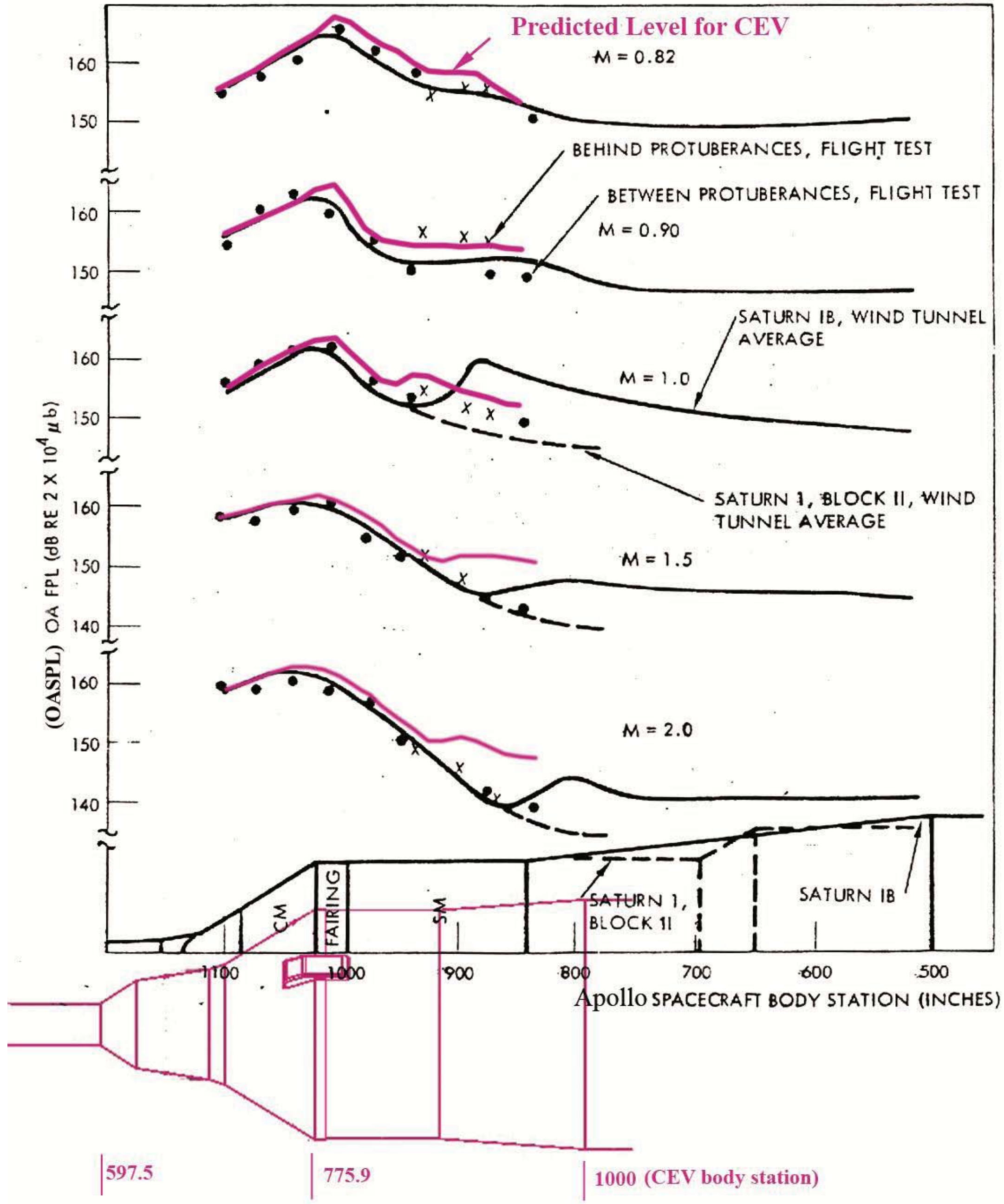

- Falls apart when vehicle shape changes

Wind tunnel tests and scaling Laws

Space Launch System (SLS) test at NASA Ames Unitary

Table 17. Rigid buffet model scaling laws.

Quantity to be Scaled	Full-scale to Model-scale Relation
Pressure	$P_{fs} = P_{ms} \frac{Q_{fs}}{Q_{ms}}$
Force	$F_{fs} = F_{ms} \frac{Q_{fs}}{Q_{ms}} \left(\frac{D_{fs}}{D_{ms}}\right)^2$
Time	$T_{fs} = T_{ms} \frac{D_{fs}}{D_{ms}} \frac{V_{ms}}{V_{fs}}$
Frequency	$f_{fs} = f_{ms} \frac{D_{ms}}{D_{fs}} \frac{V_{fs}}{V_{ms}}$
Pressure PSD (psi^2/Hz)	$\phi_{fs}^{(P)} = \phi_{ms}^{(P)} \left(\frac{Q_{fs}^{(P)}}{Q_{ms}^{(P)}}\right)^2 \frac{D_{fs}}{D_{ms}} \frac{V_{ms}}{V_{fs}}$
Force PSD (lbf^2/Hz)	$\phi_{fs}^{(F)} = \phi_{ms}^{(F)} \left(\frac{Q_{fs}^{(F)}}{Q_{ms}^{(F)}}\right)^2 \left(\frac{D_{fs}}{D_{ms}}\right)^5 \frac{V_{ms}}{V_{fs}}$

What to do if measured fluctuations are very high? – cost and weight penalty

Real Engineering – What if the acoustic levels are too high?

MPCV Shape Optimization to Reduce Aero-acoustic environment

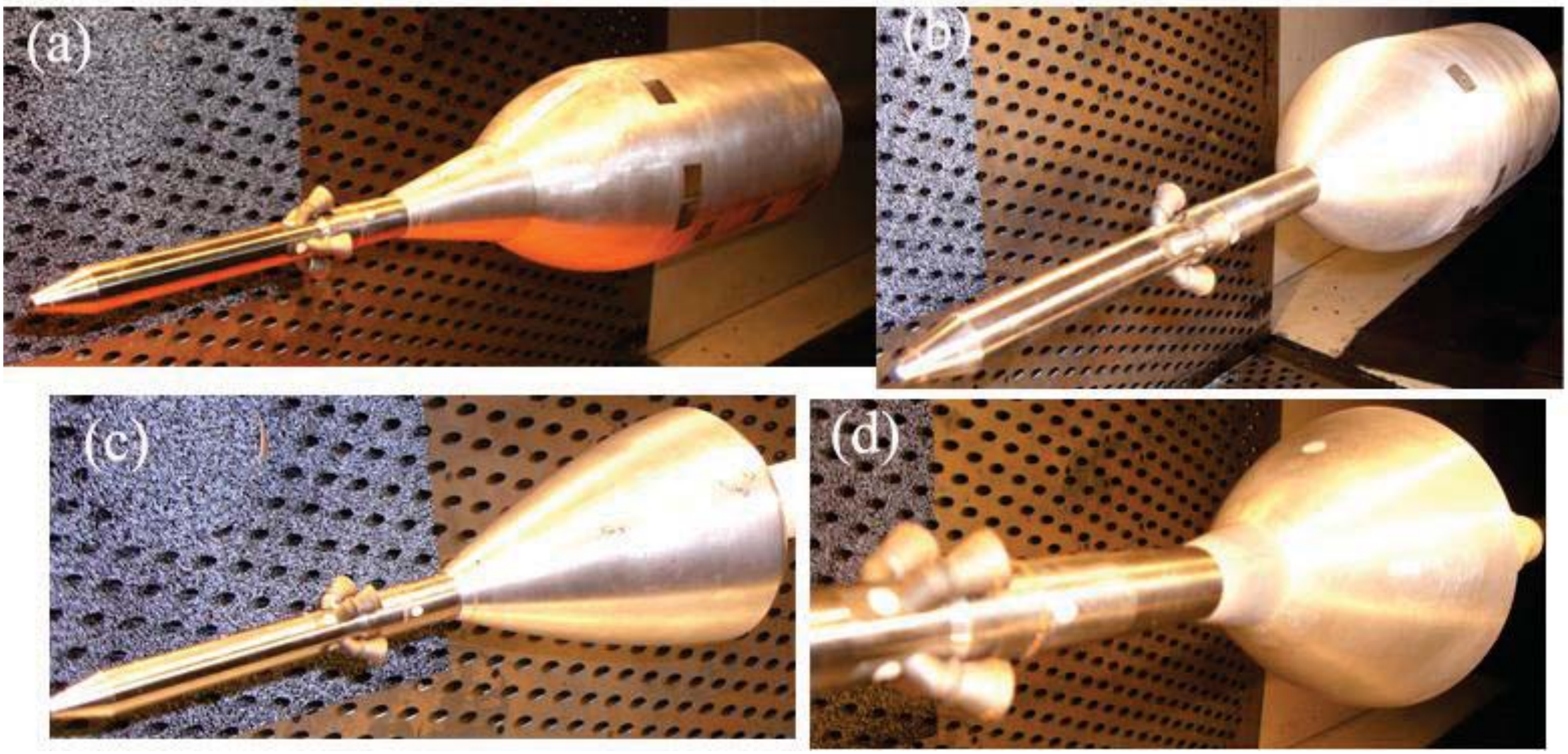

MPCV Shape Optimization to Reduce Acoustic environment

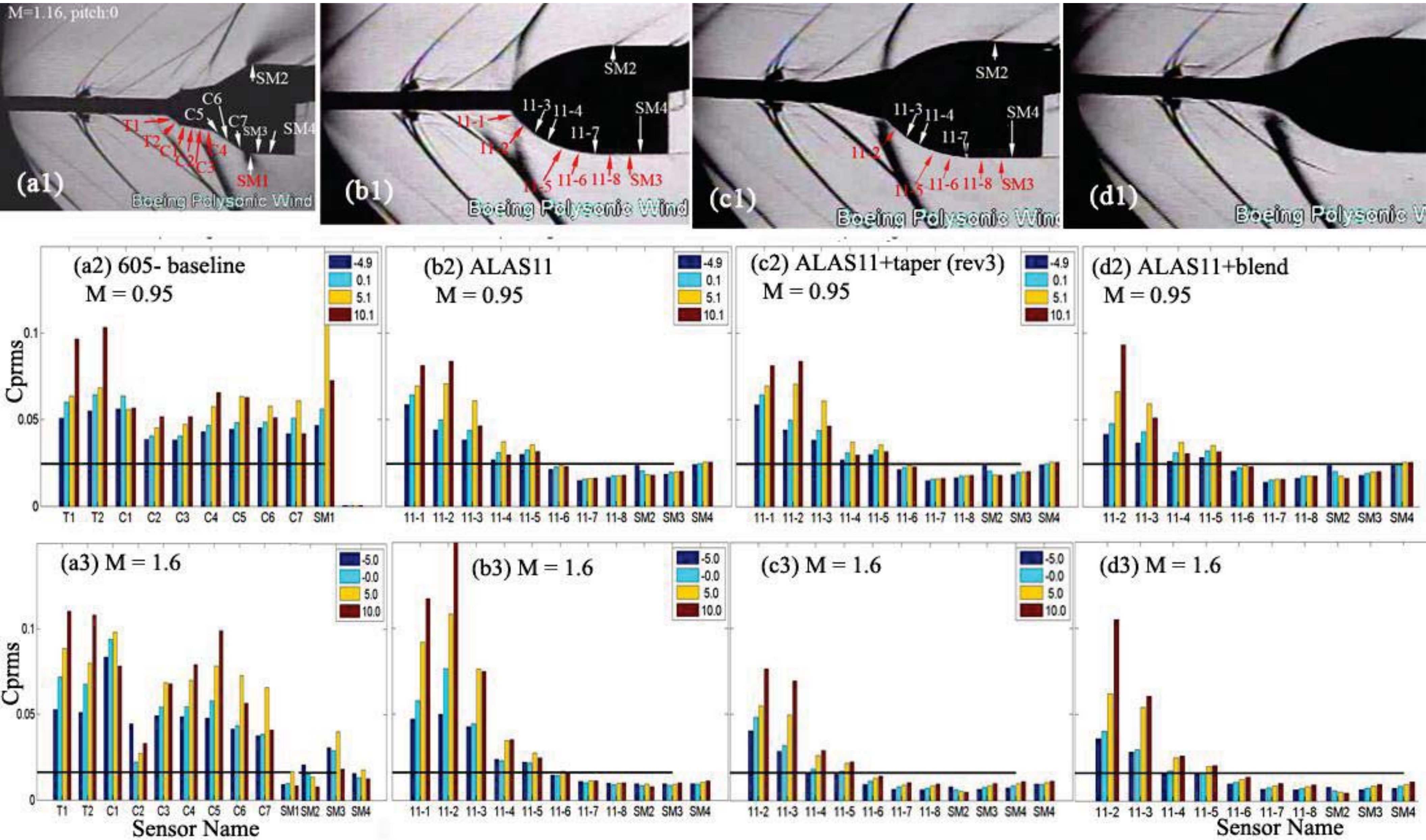

MPCV Shape Optimization to Reduce Acoustic environment

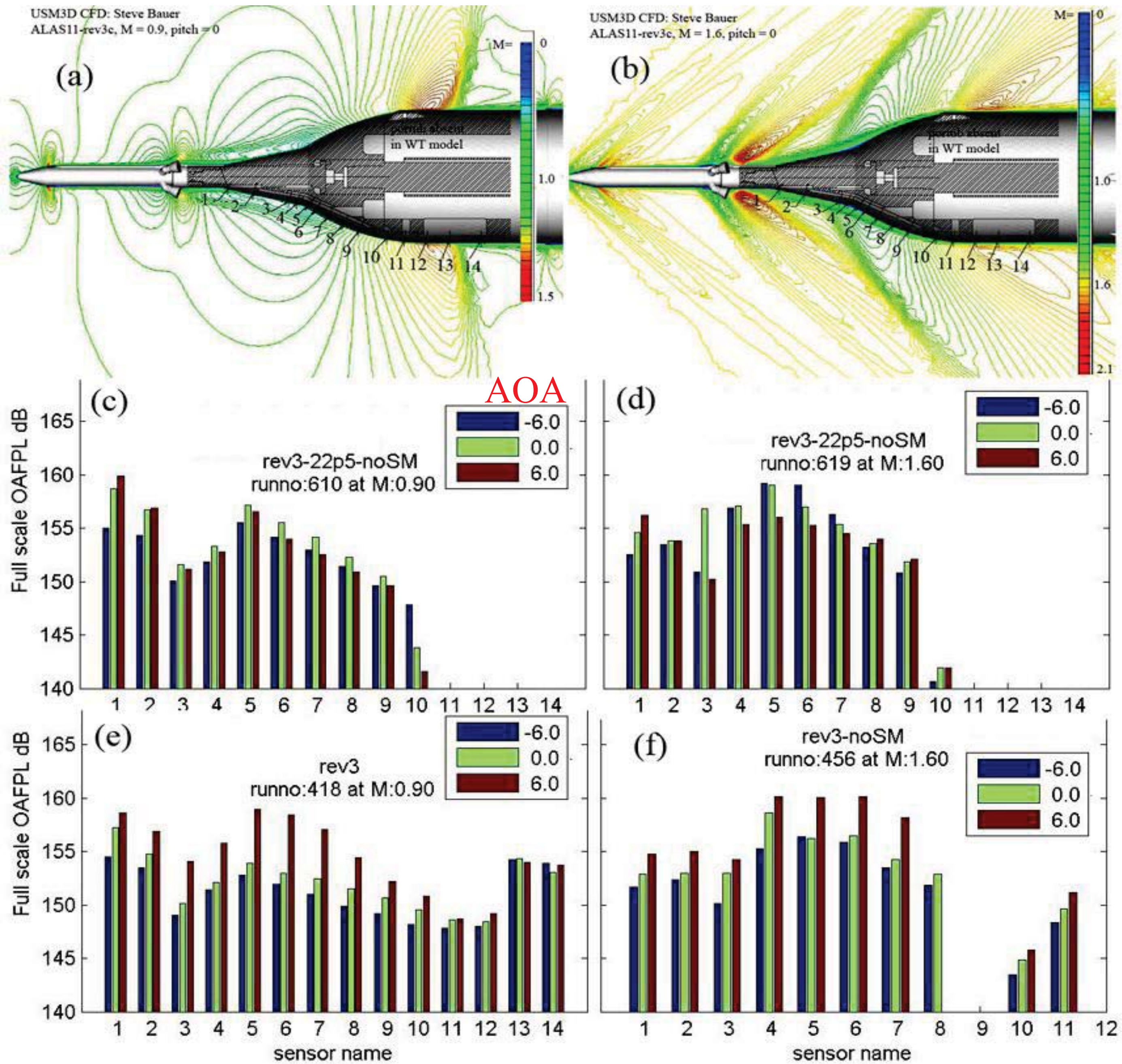

Comparison with Data from Flight Test – ARES-IX

Reed et al. AIAA 2011-174

Fig. 6 Transducers OAD819P, OAD920P, OAD921P, and OAD922P locations.

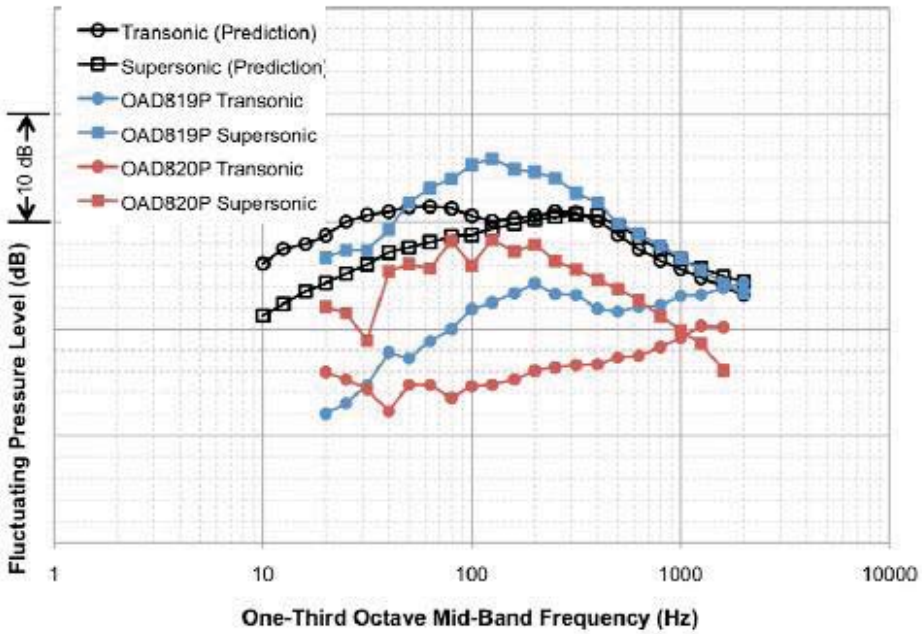

Fig. 9 Transducer OAD827P location.

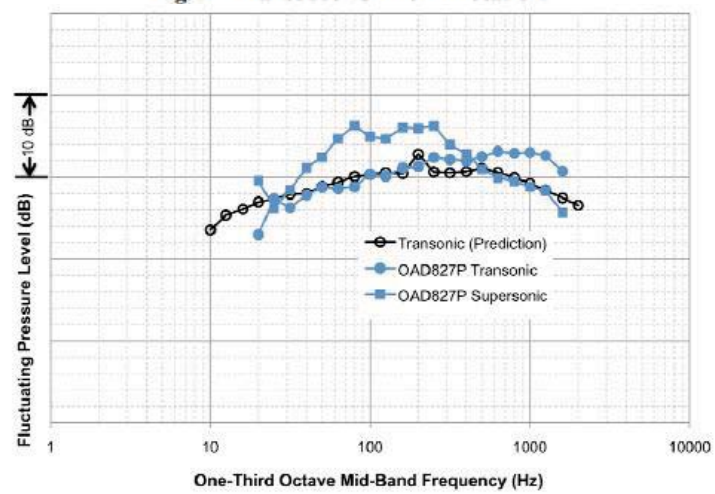

- In general reasonable comparison
- Discrepancies near changes in outer mold line geometries.
- zones near protuberances show poor comparison
- Data from supersonic part of the flight show poor comparison
- Flaws in the scaling laws?? Reynolds number effect?

Buffet:

- Coupling between global bending and/or torsional modes of the vehicle with unsteady separated flow.
- Frequently associated with unsteady shock motion at transonic M
- Low freq <20Hz
- May lead to catastrophic failures
- Estimation of Buffet forces via integrating pressure fluctuations

Abort Acoustics
o Problem definition
o Wind tunnel simulation, CFD
o Flight test

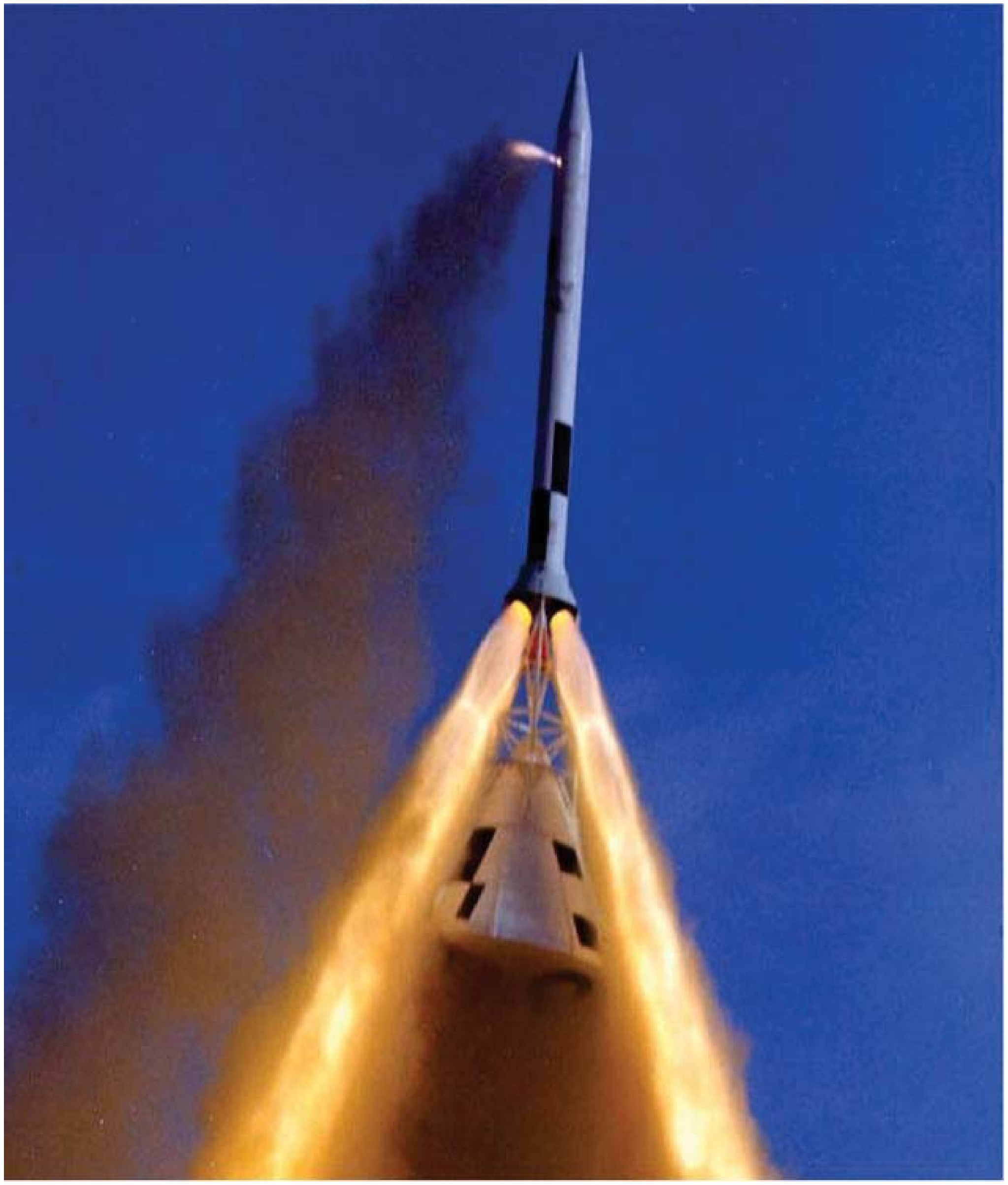

Apollo Abort test

ORION/MPCV and the Launch Abort System

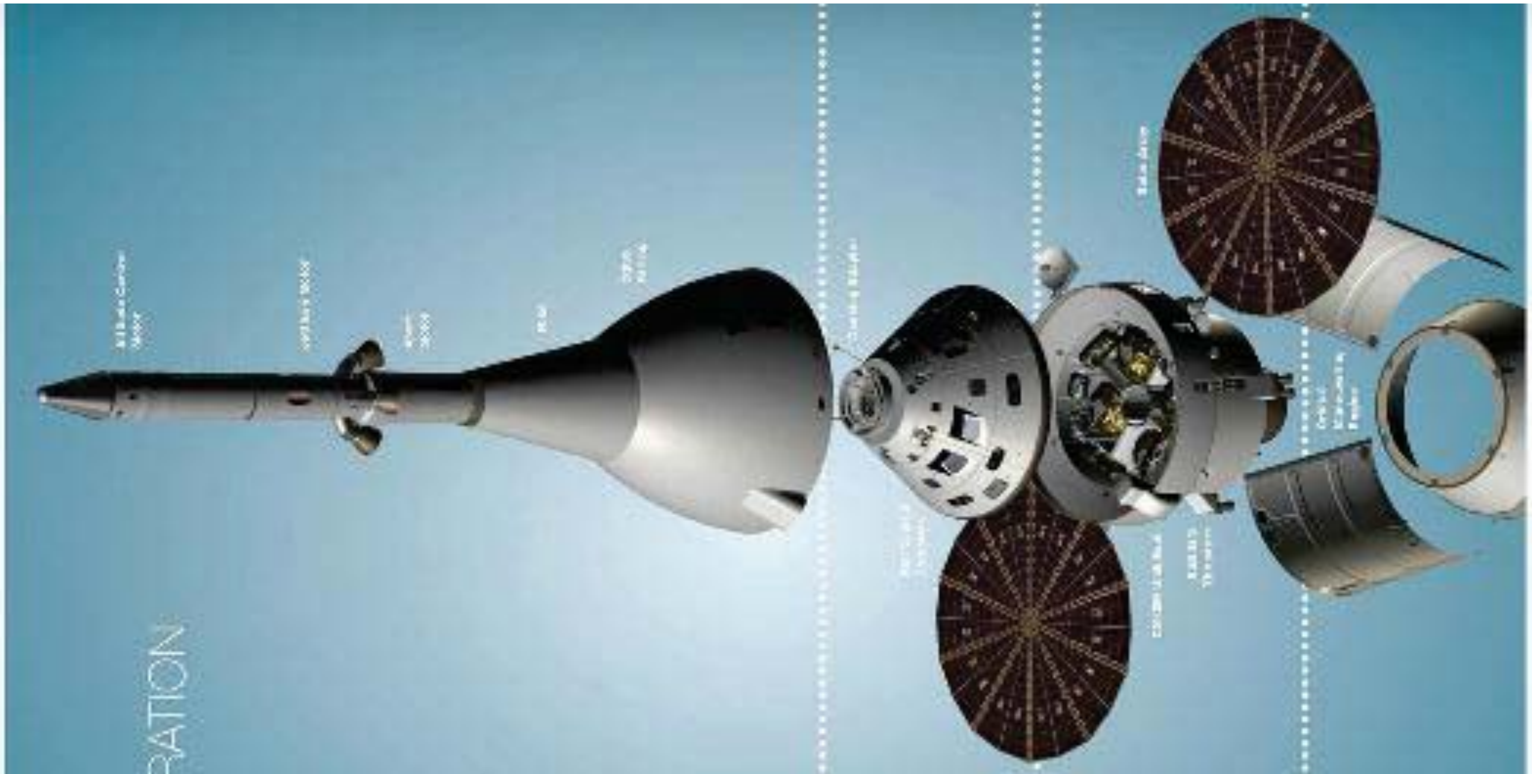

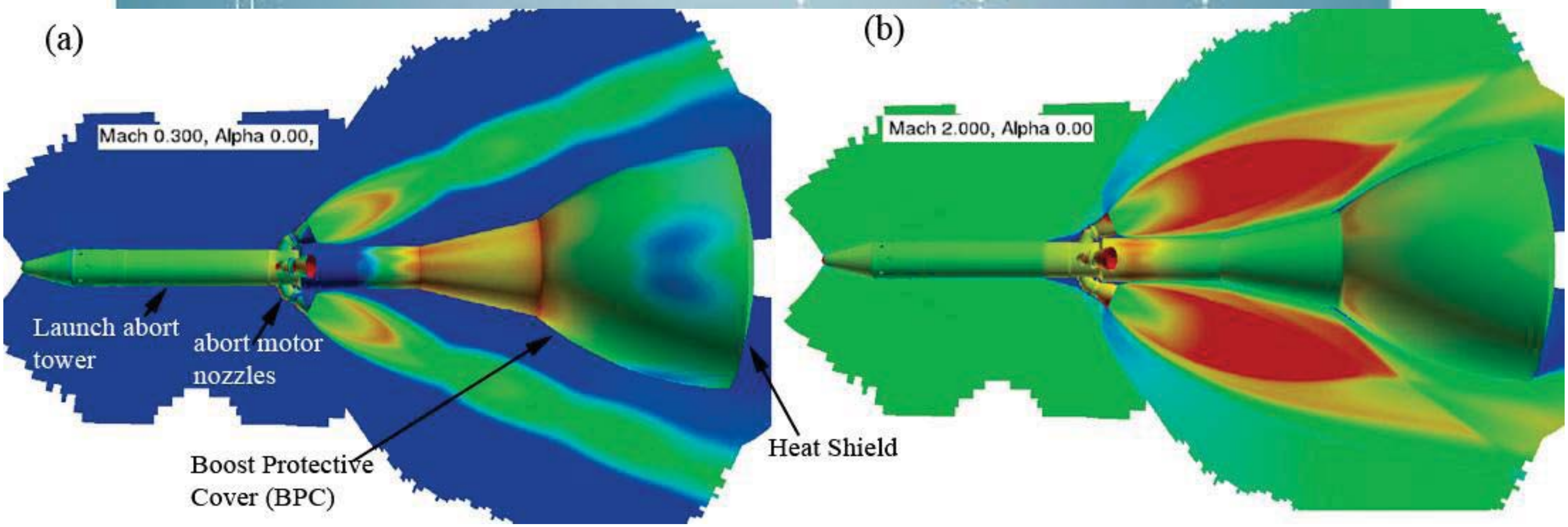

Prediction –

- Initial prediction Based on SP-8072 – Not dependable

- No prior experience from Mercury or Saturn programs
- All microphones burnt out in one flight test

Measurement of plume-generated noise in the static test of MPCV launch abort motor ST1

Results from ST1

Abort Acoustics

- No prior aerospace structure was subjected to this high level of dynamic load

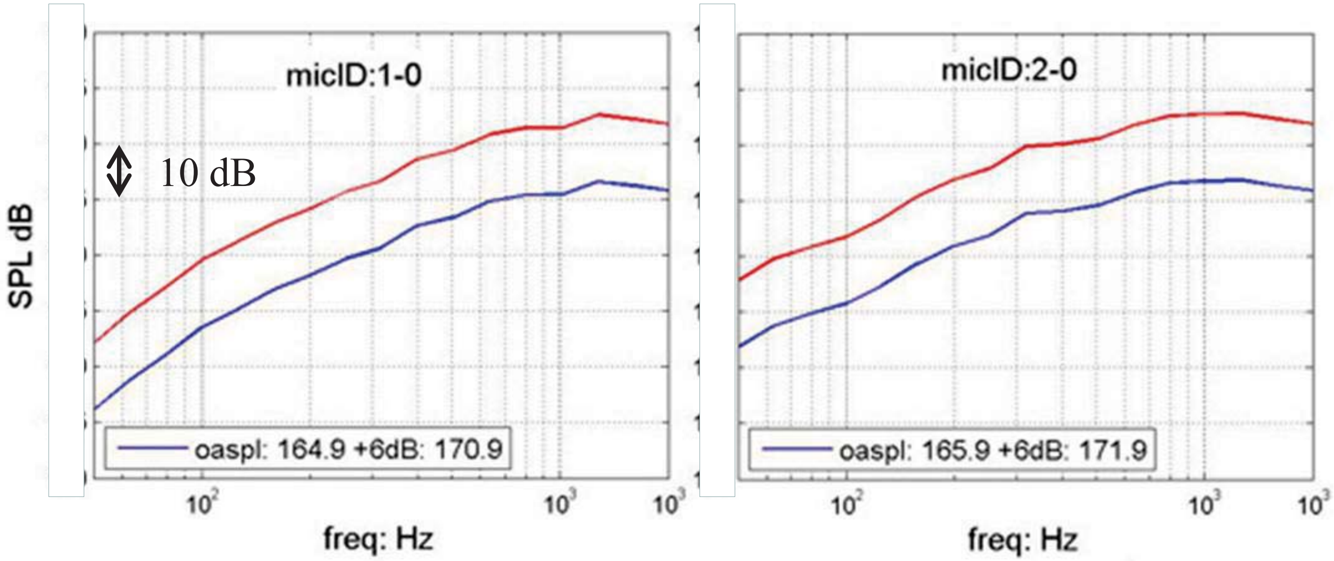

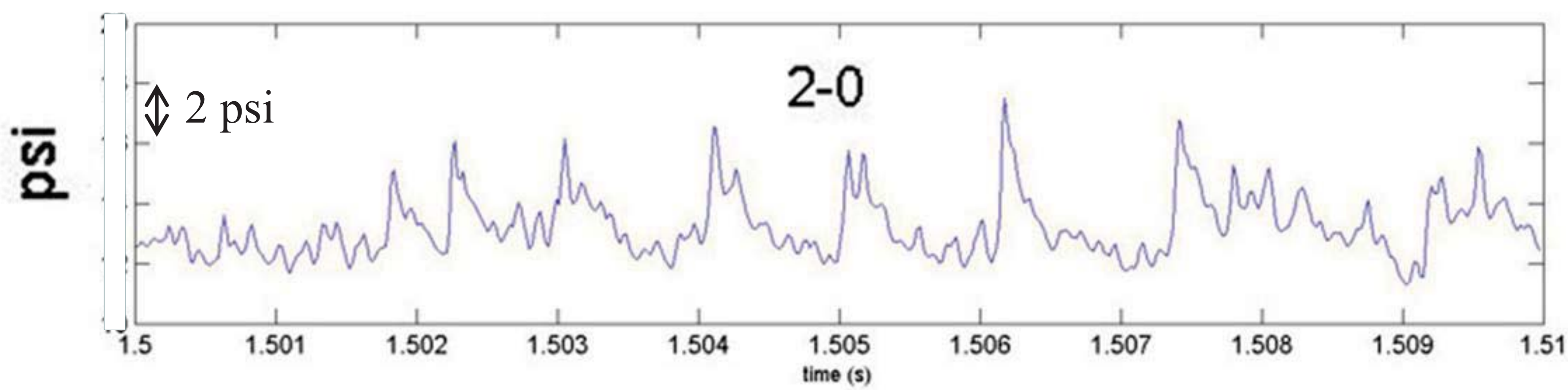

Very high level
High freq dominated
Non-linear, shock dominated

How to create acoustic environment for Abort?

- Single flight tests are unsuitable to create a design environment
- we needed to know levels over $0 \leq M \leq 4$ and $10° \leq \alpha, \beta \leq -10°$
- Requires transonic supersonic wind tunnel to simulate forward flight

Why hot-Helium?

- Hot He reproduces acoustically relevant parameters:

  speed of sound, velocity, density.

  Pressure fluctuations at a point **X** on LAV (Ffowcs-Williams,1965):

$$p(\mathbf{X},\tau) = \frac{1}{2\pi}\int_V \frac{\partial^2 \mathbf{T}_{ik}}{\partial Z_i \partial Z_k}\left(\mathbf{Z},\tau - \frac{r}{c}\right)\frac{d\mathbf{Z}}{r} \quad (1)$$

$$\mathbf{T}_{ik} = \rho u_i u_k + \delta_{ik}(p - c^2\rho) \quad (2)$$

- Validation from prior small-scale tests:

  SRM vs. He: Morgan & Young (1963)

  Jet engine noise: Doty & McLaughlin (2001), Kinzie & McLaughlin (1999)

  Papamoschou (2007), Greska & Krothapalli (2009)

- Practicality of operation:
  - Suitable in a wind tunnel .
  - Use of high fidelity model with all 4 nozzles.
  - Survivability of the kulite sensors
- Cost effective means of creating 80 abort conditions.

- Primary differences between He and rocket plume:
  - Lack of afterburning;
  - Absence of Al_2O_3 particles;
  - Different γ

Matching between wind tunnel and flight conditions

$$\frac{p_f'}{p_t'} = f\left(\frac{D_{er}}{D_{eh}}, \frac{D_{jr}}{D_{jh}}, \frac{\alpha_r}{\alpha_h}, \frac{\beta_r}{\beta_h}, \frac{M_{jr}}{M_{jh}}, \frac{M_{er}}{M_{eh}}, \frac{(p_e/p_a)_r}{(p_e/p_a)_h}, \frac{c_{jr}}{c_{jh}}, \frac{\rho_{jr}}{\rho_{jh}}, \frac{\rho_{er}}{\rho_{eh}}, \frac{U_{jr}}{U_{jh}}, \frac{U_{er}}{U_{eh}}, \frac{(J_e/J_a)_r}{(J_e/J_a)_h}, \frac{W_{er}}{W_{eh}}, \frac{q_f}{q_t}, \frac{q_{jr}}{q_{jh}}\right) \quad (7$$

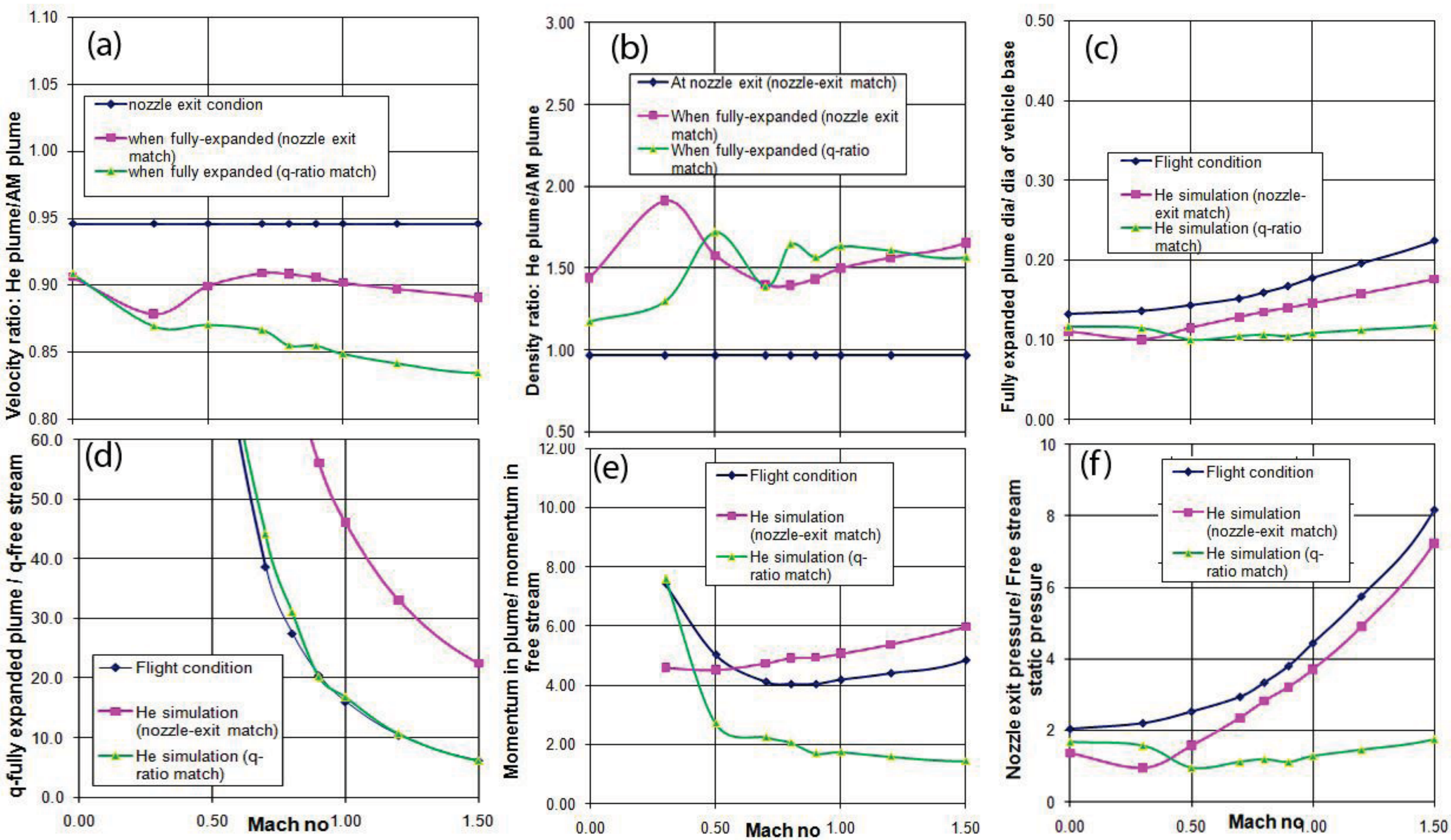

Abort initiated at M 1.6 : Influence of forward flight

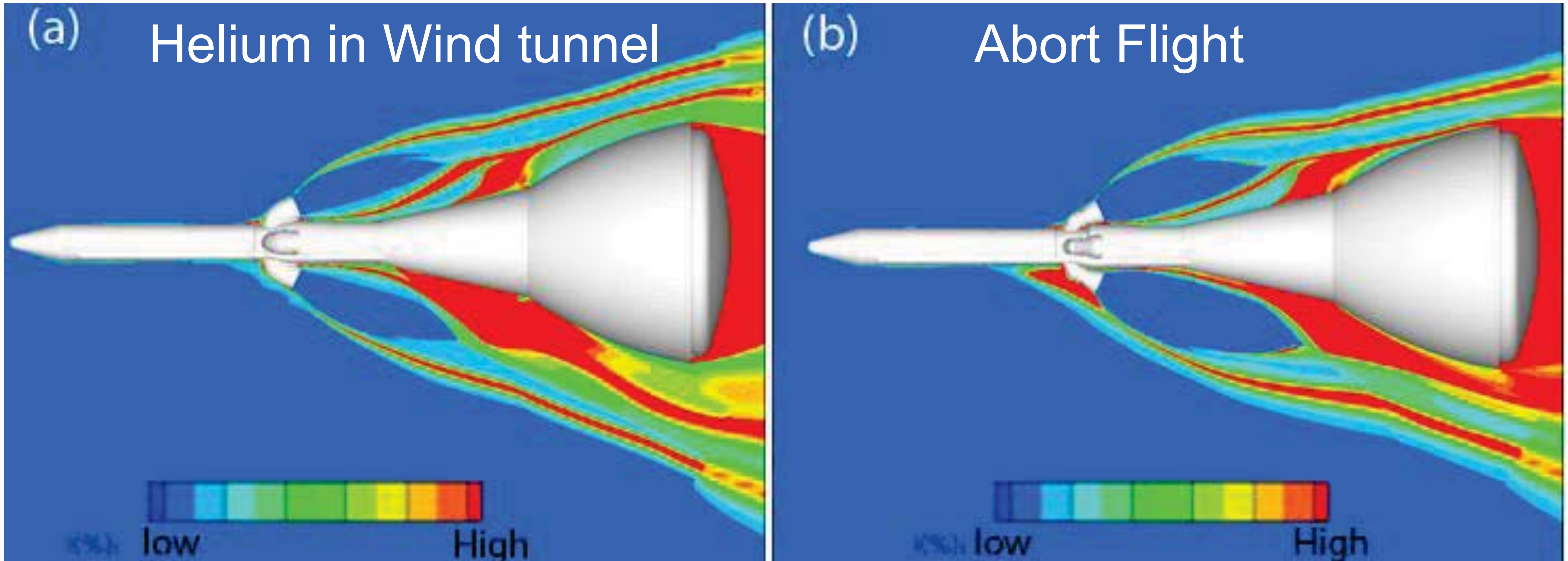

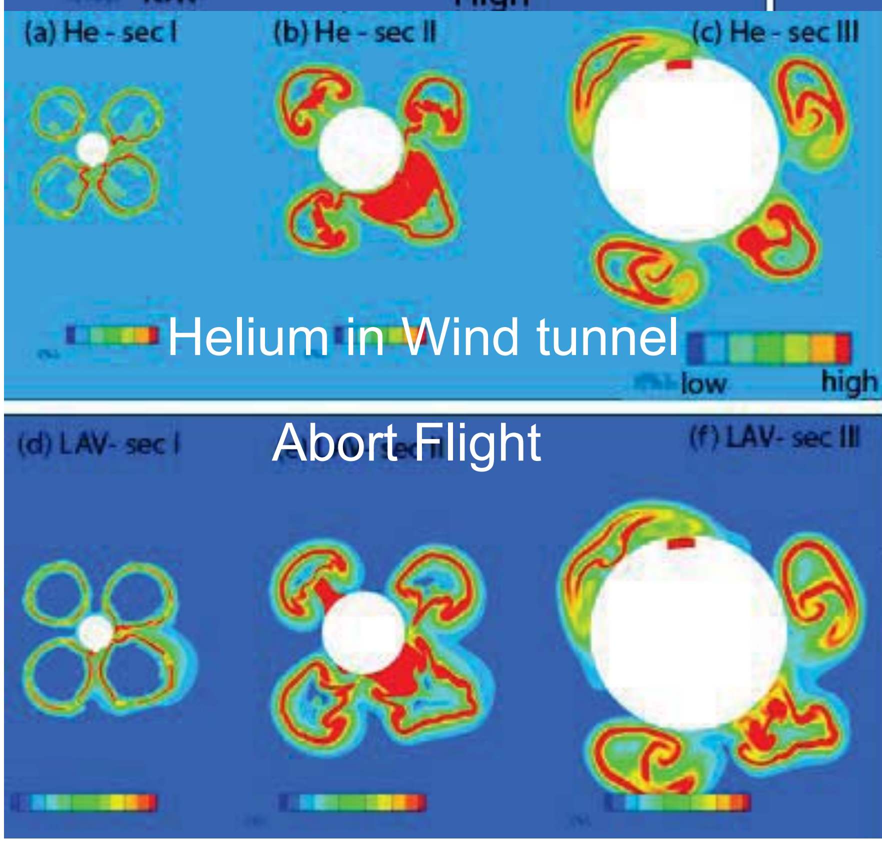

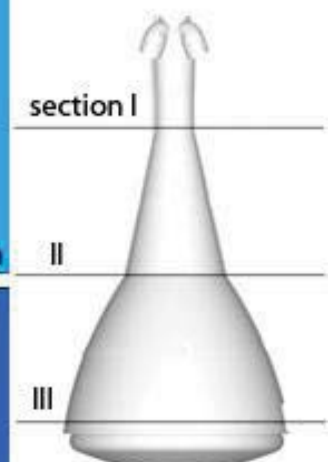

Distribution of turbulence intensity

$M_a = 1.6$, $\alpha = -10°$, $\beta = -10°$

CFD by: William J. Coirier, Kratos/DFI

Abort initiated at M 1.2 : Influence of forward flight

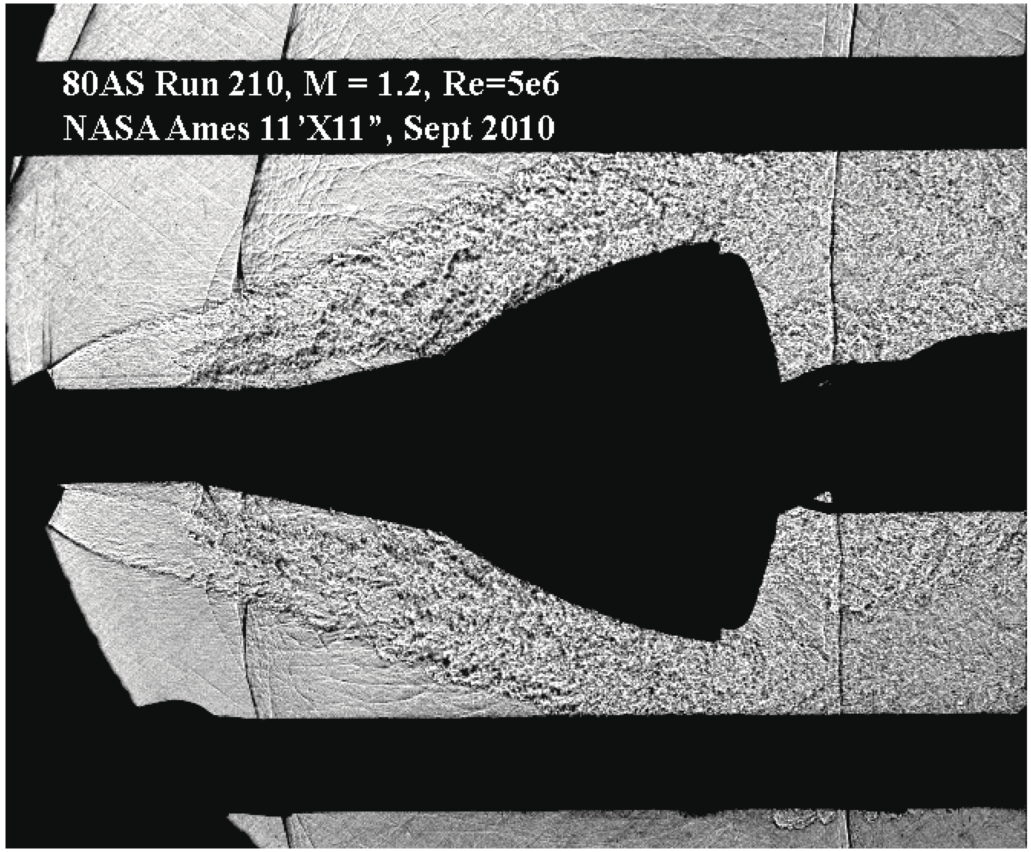

- Wind tunnel pressure fluctuations need to be scaled to flight condition
  - problem of two different ratios of dynamic pressures:

$$\frac{p'(\text{model})}{p'(\text{flight})} = f\left(\frac{\text{Dynamic press tunnel}}{\text{Dynamic press flight}}, \frac{\text{Dynamic press Helium plume}}{\text{Dynamic press Rocket plume}}\right)$$

► Each abort condition was simulated by two Helium + Wind tunnel setup:
- Nozzle exit match
- q-ratio match

Run Matrix – Test Conditions

- **Test conducted in the NASA Ames 11-Ft Unitary Plan wind tunnel**
- **Mach Range** 0.3 – 1.2
- **Reynolds Number:** $2x10^6$ - $5.0x10^6$/foot,
- He pressure at Model Plenum: 300psi to 600psi
- He temperature at Model Plenum: 660F to 700F
- Internal piping for 11 different model attitudes:

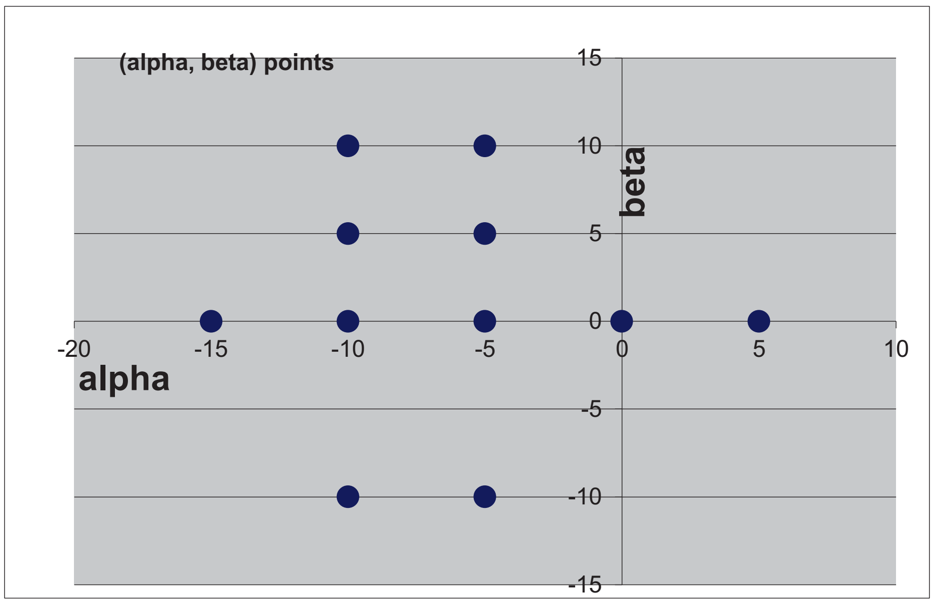

Abort Acoustics

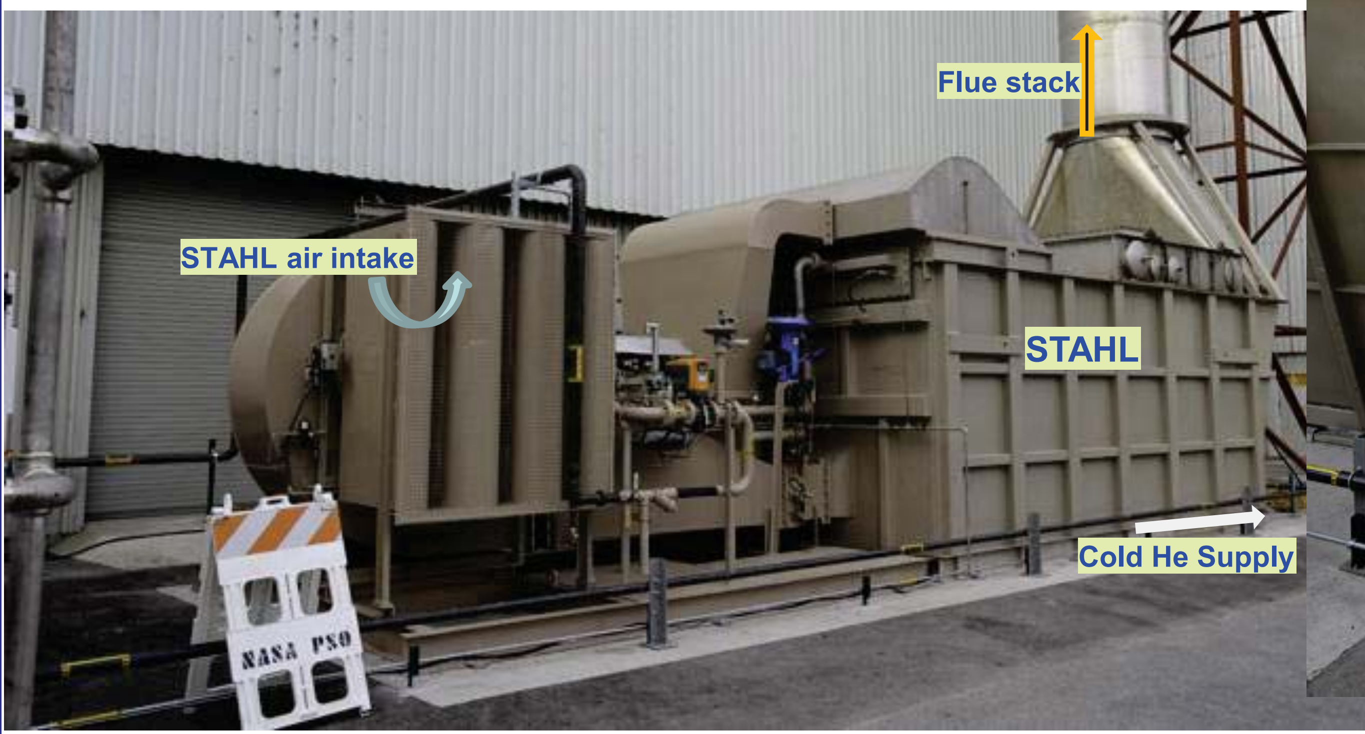

Abort Acoustics

Model and Instrumentation

Abort Acoustics

- 6% scaled of LAV 606 F.1
- Continuous active cooling of the model core
- Subjected to very large temperature cycle – periodic heating and cooling.
- 237 Kulite sensors

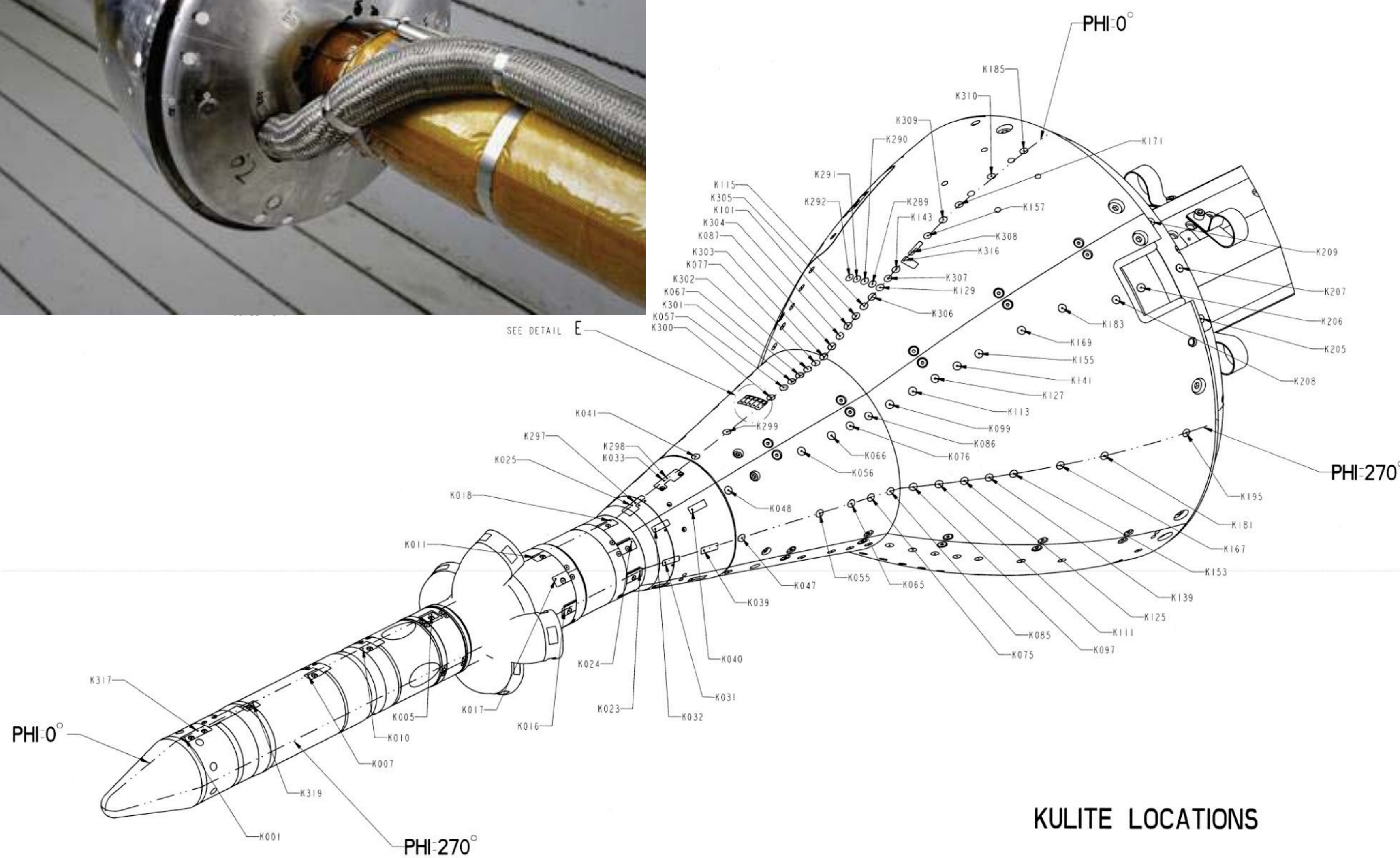

Sample Result: Run 184: M = 0.3, Re = 3e6, α=0, β=0

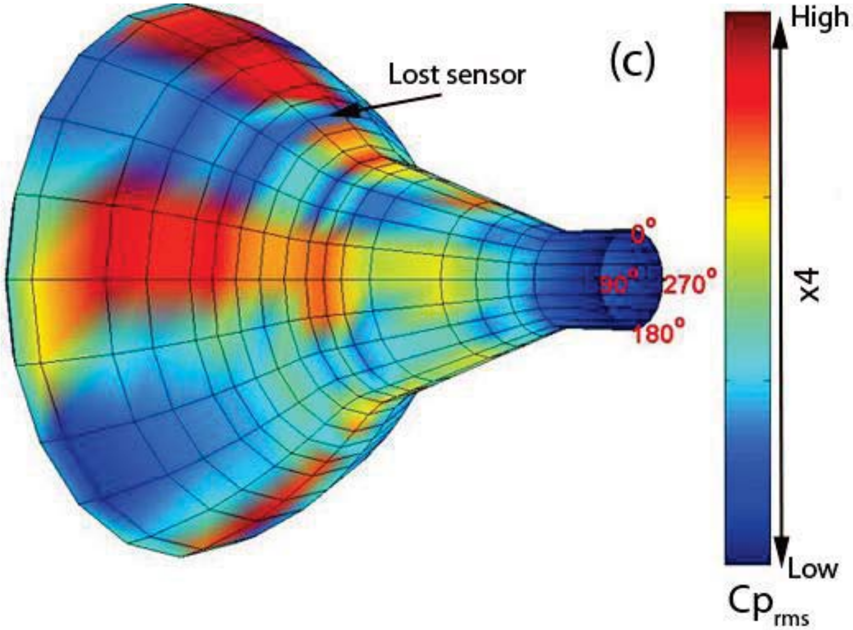

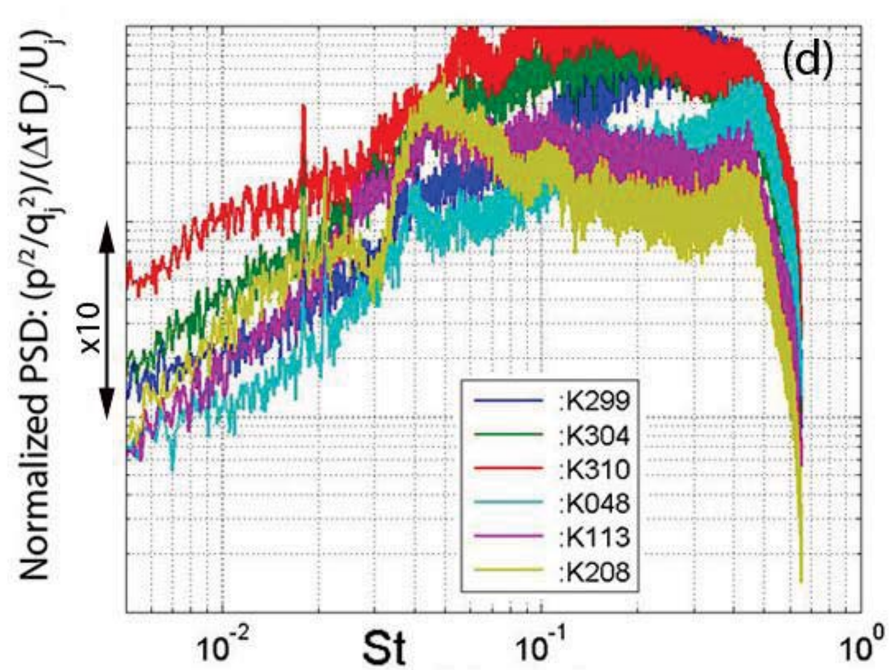

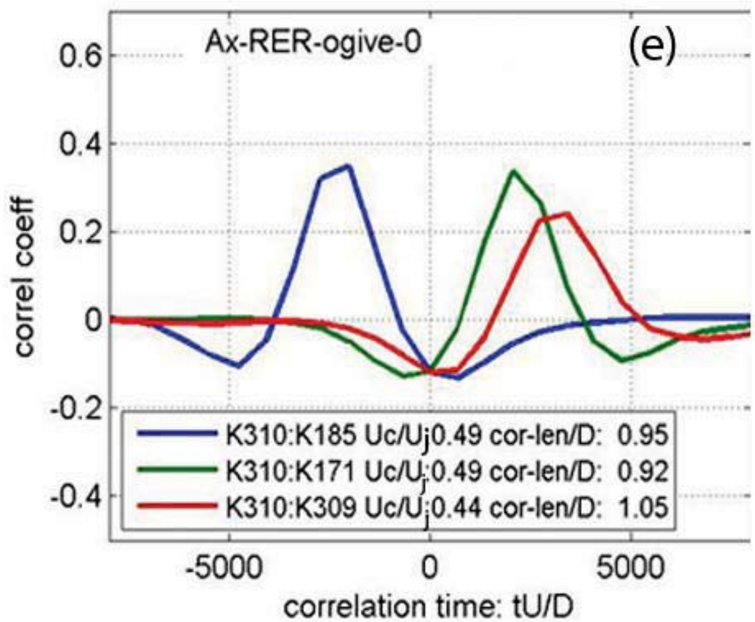

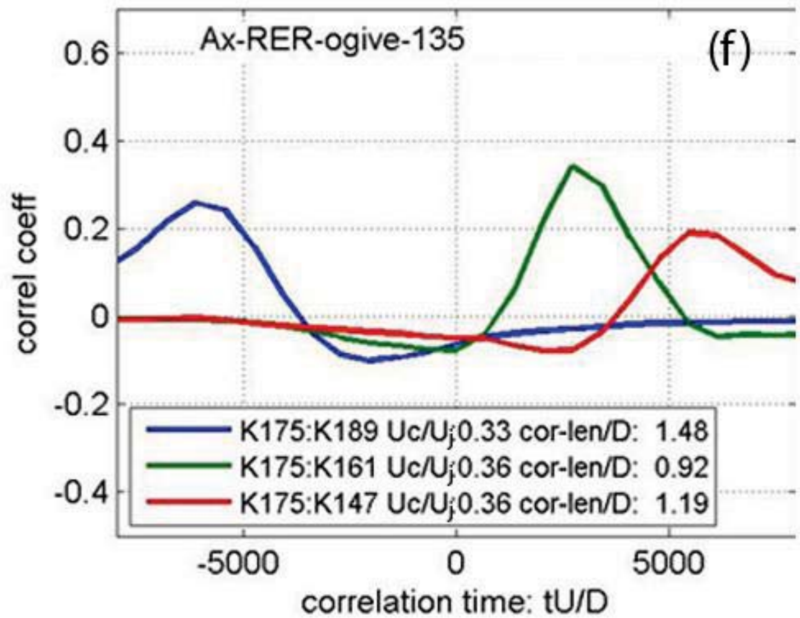

Effect of Forward Flight

M = 0.3

M = 0.6

M = 1.2

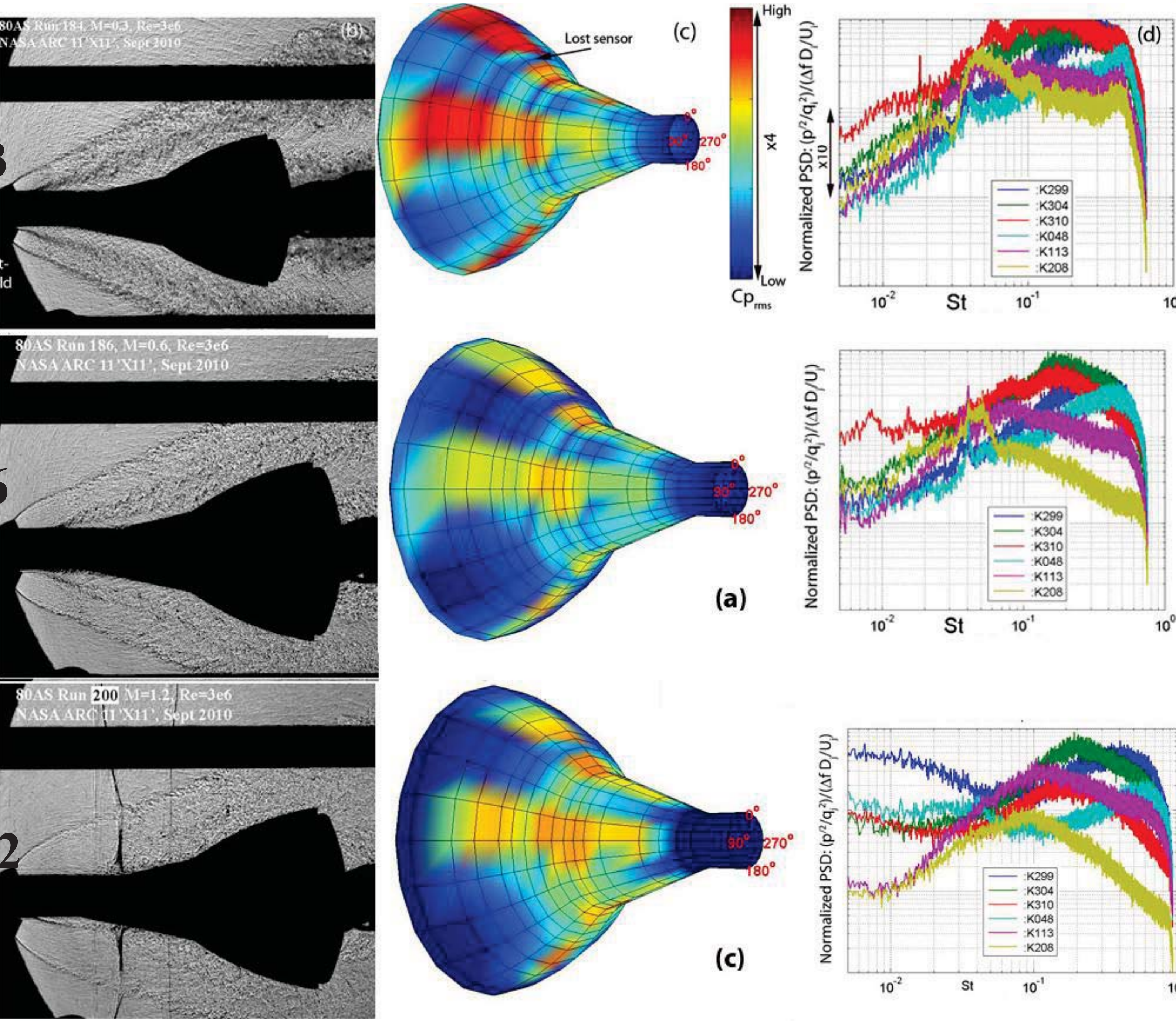

Jay Panda (ARC-AOX) 650-604-1553

Abort Acoustics

July 2010

Pad Abort-1 is a NASA flight test of a system that could be used to rescue a crew and its spacecraft in case of emergencies at the launch pad.

www.nasa.gov

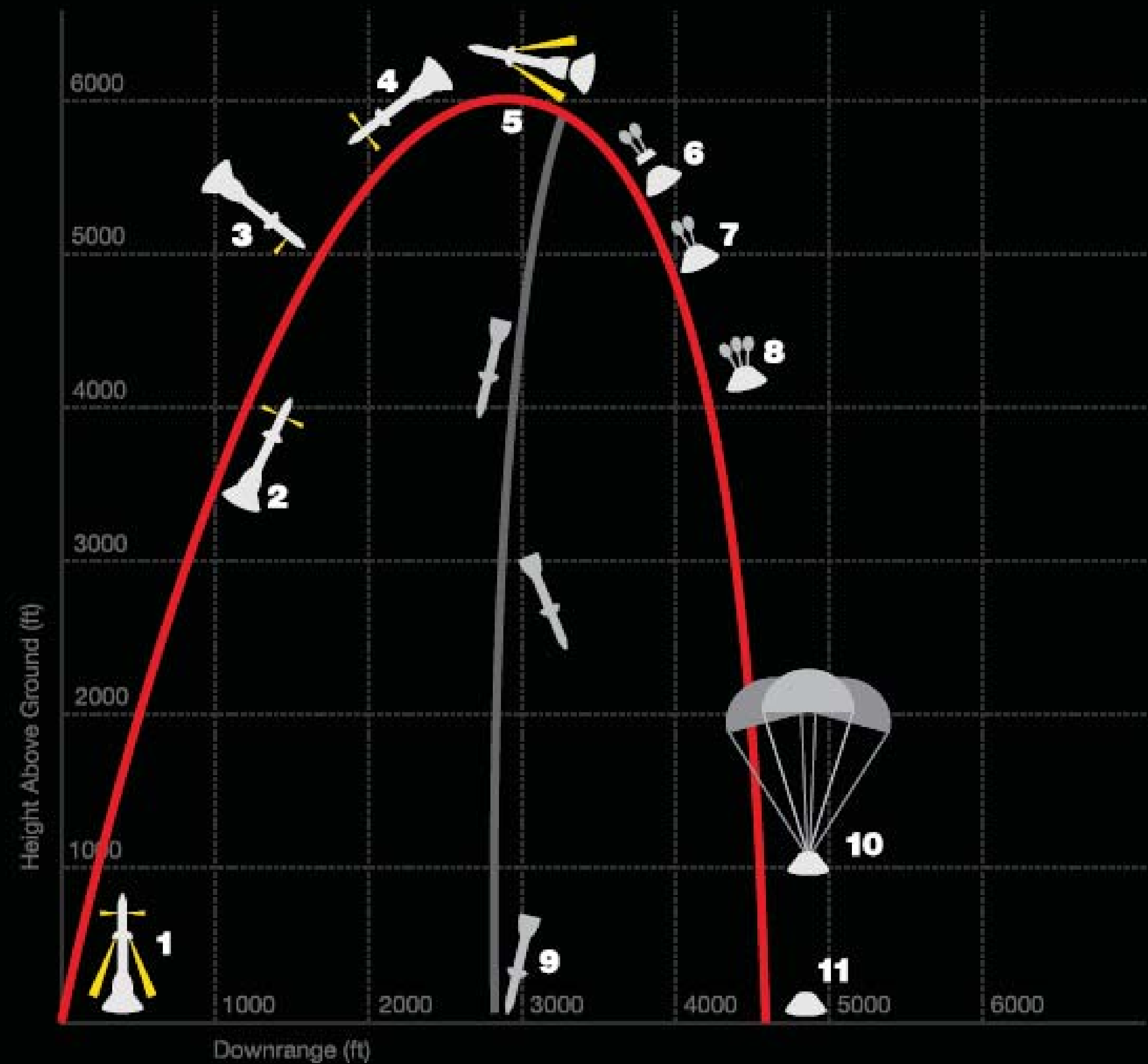

Abort Acoustics

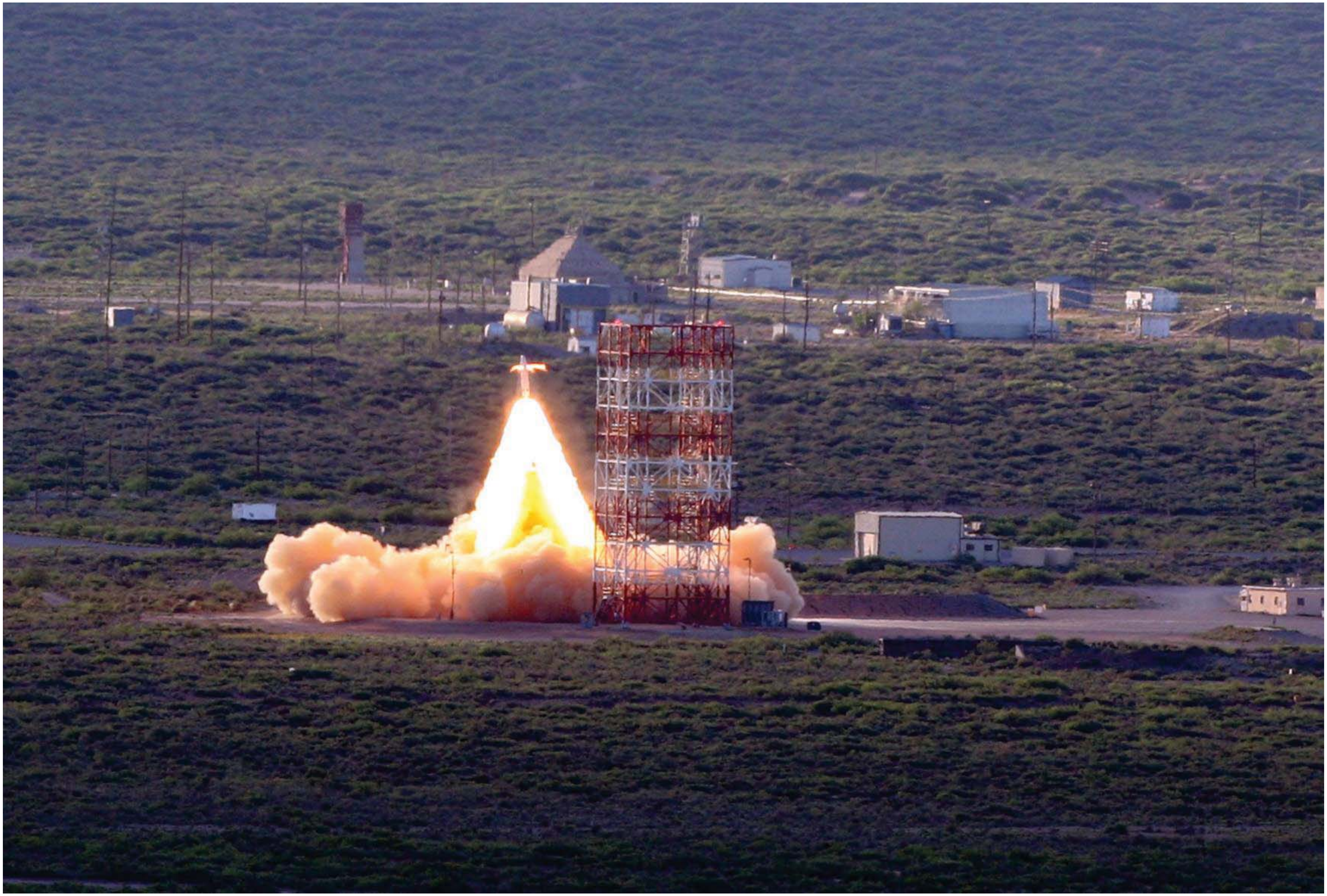

Comparison with Pad Abort 1 flight data

Pad Abort test flight PA1:

- ○ Happened on July 2010 from White Sands
- ○ Full scale unmanned flight vehicle, old Mold Line,
- ○ accelerated from M 0 to ~ 0.7 over the burn duration.
- ○ 57 sensors distributed over lower tower and Party-hat

- ● **Not exactly apple-to-apple comparison**
- ○ Older, slimmer profile
- ○ ***Flight:*** transient data, ***wind tunnel:*** steady state
- ○ Wind tunnel: No Attitude Control Motor

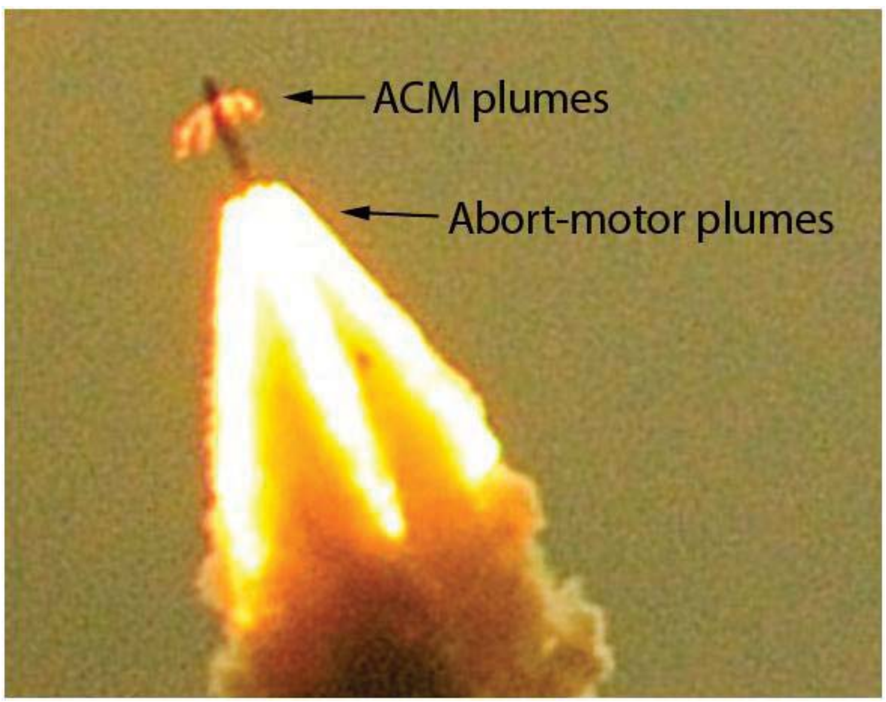

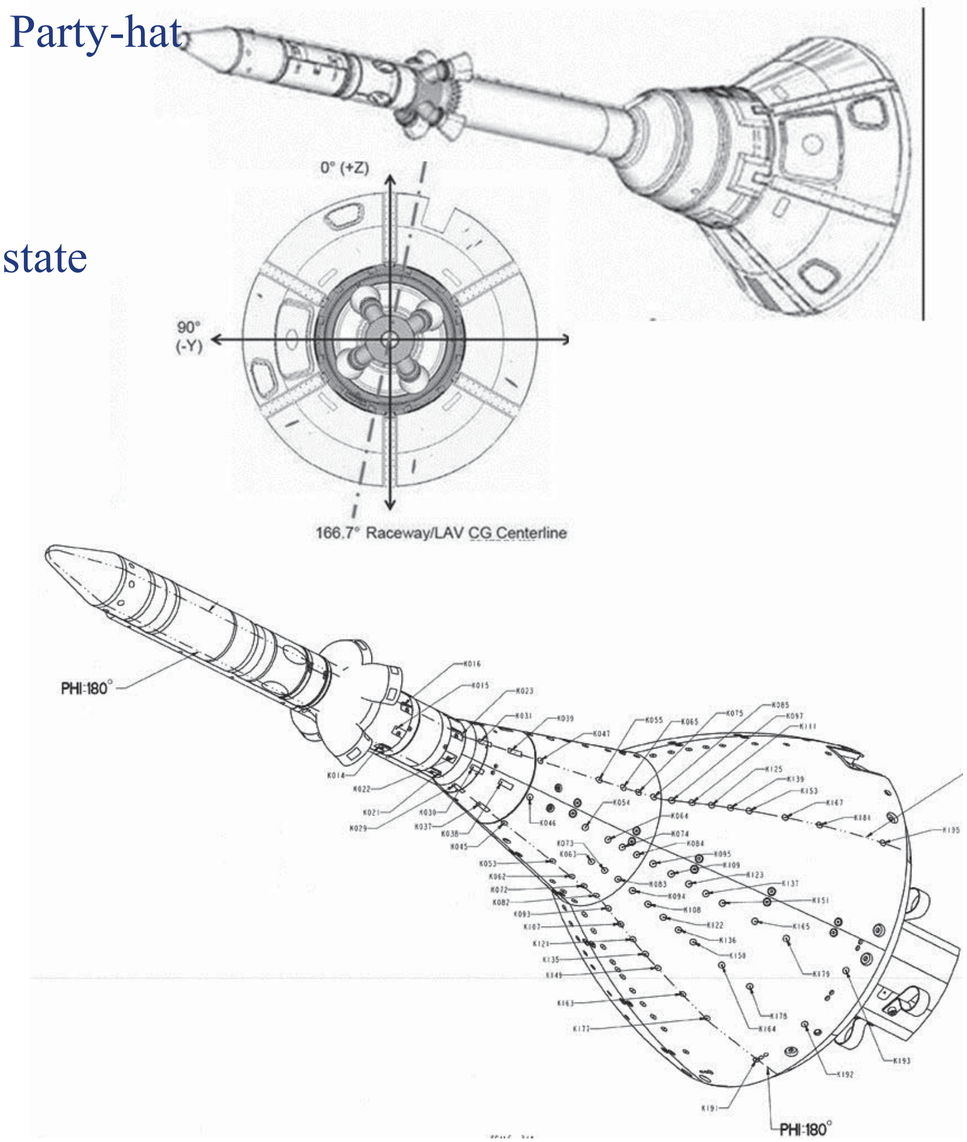

Comparison with PA1 flight data

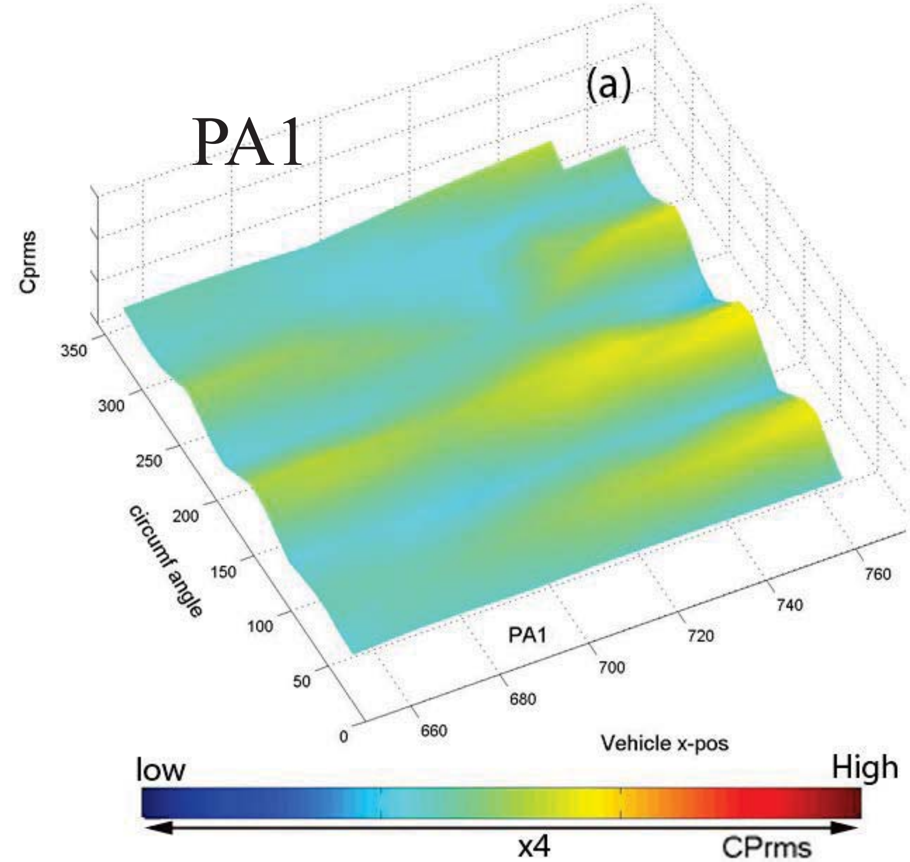

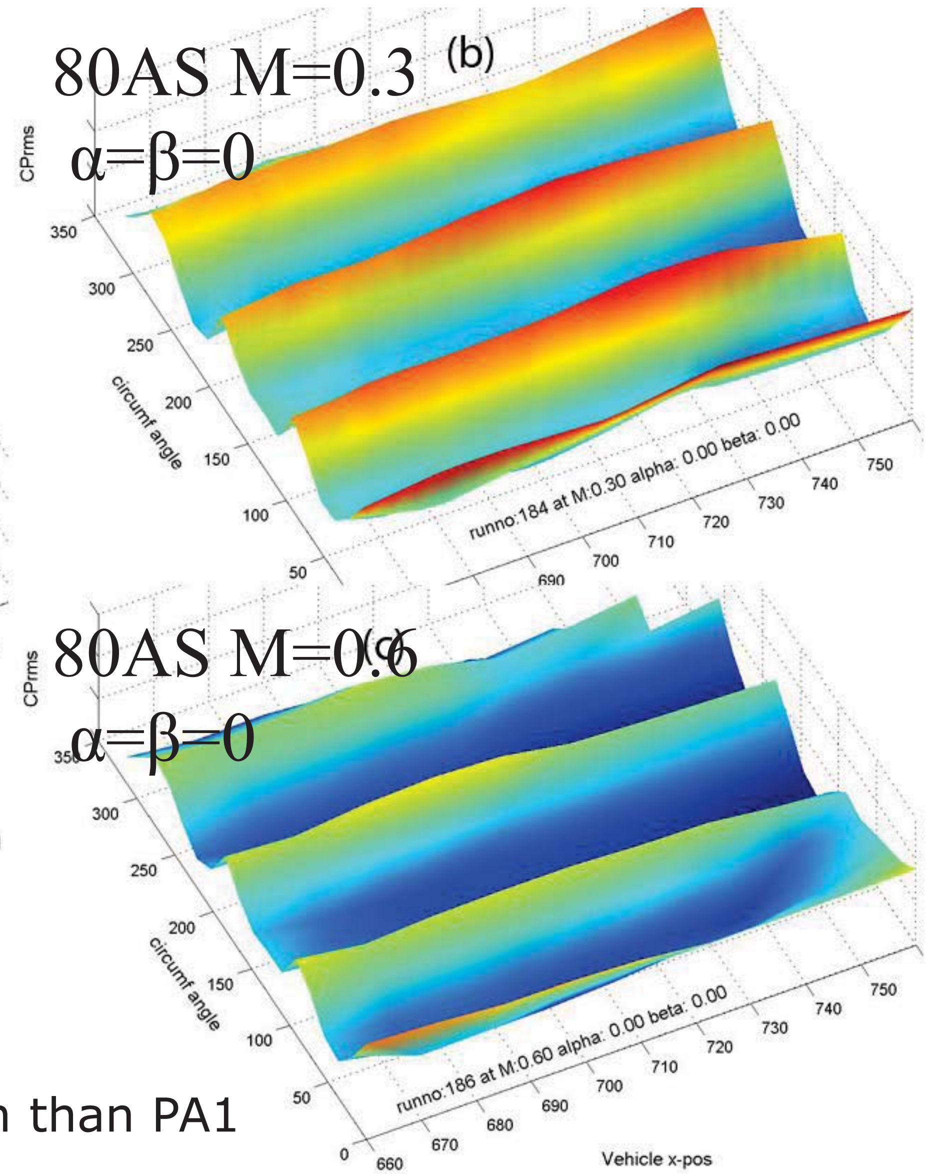

- 80AS show wider crest-trough variation than PA1
  - PA1 flew with non-zero α, β
  - PA1 had ACM induced turbulence

Comparison with PA1 flight data – q scaling

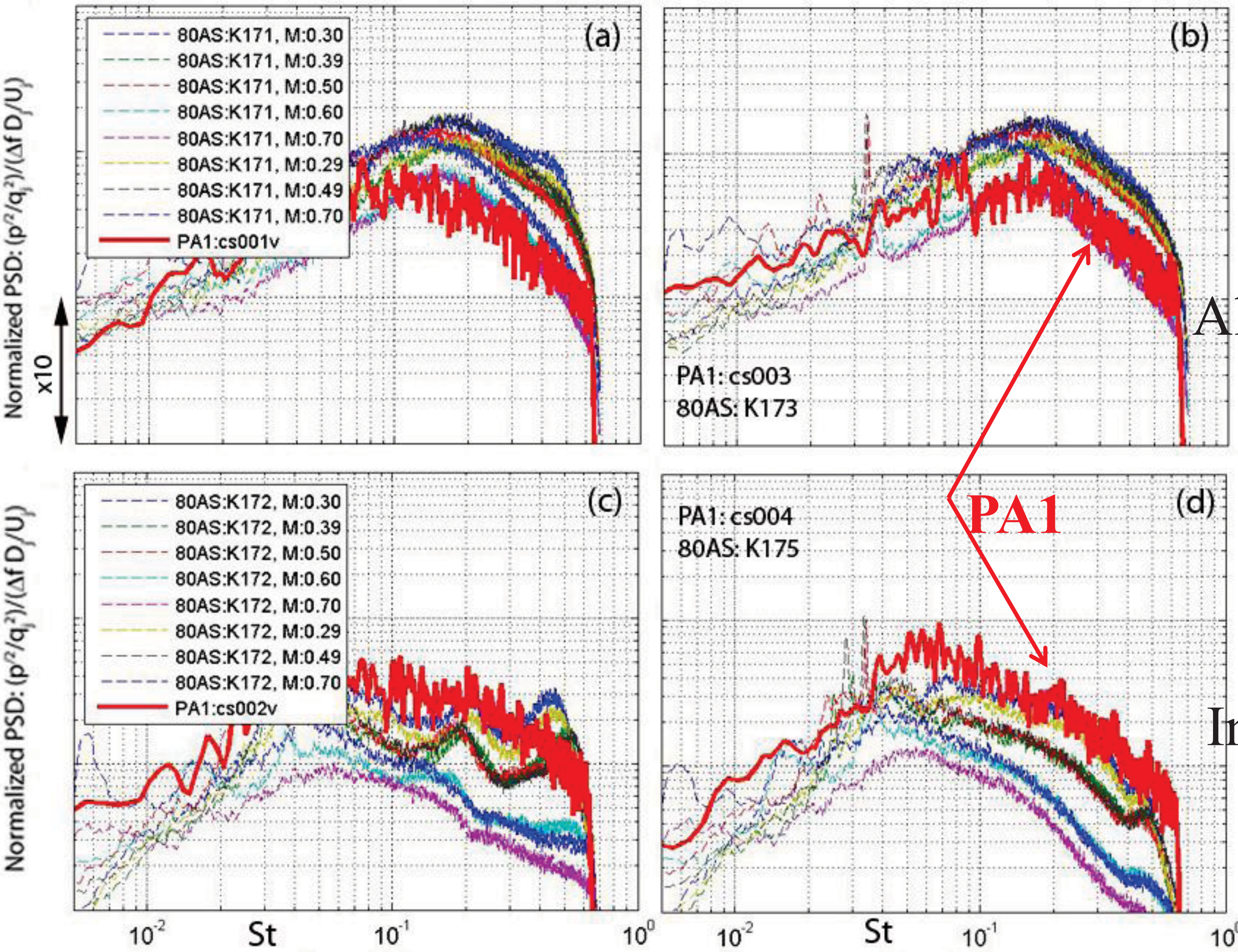

Along Plume axes

In Between Plum

Existing uncertainties:

- Scaling laws for abort initiated at transonic/supersonic flight
- Increment in environment due to scattering of plume by vehicle induced shock waves

Expecting further validation from another flight test

- Ascent Abort 2 (AA2) – Abort initiated at M ~ 1.1

Summary:

Basics

- For launch vehicles aeroacoustics is a part of fluid-structure interaction problem
- Separation into Aeroacoustics and Vibro-acoustics
- Aeroacoustics = surface pressure fluctuations
- Forcing functions for vibro-acoustic calculations
  - overall level – extremely high
  - auto-spectra
  - cross-spectra
- Need for direct solution of fluid-structure interaction.

Launch Acoustics

- Complexity of launch pad – acoustic suppression systems
  - deflector and trench design
  - vehicle trajectory and drift
  - amount of water injection and timing schedule
- Prediction via NASA SP-80672 & limitations
  - ignores plume impingement, water injection, vehicle drift
- Prediction via flight data from prior launch vehicles
  - very large spread, different for a new vehicle
- Limited ability of CAA
- Use of a microphone phased array for direct identification of noise sources
  - Very different description of noise sources that SP-8072

Summary:

Ascent Acoustics

● Source- turbulent flow over vehicle surface, local flow separation, unsteady shocks
- dynamic pressure and vehicle trajectory

● Prediction – identification of local flow separation and transonic/supersonic shock wave.
- Improvement of empiricism via input from CFD
- Future need for less empiricism - CFD ?
- Data from prior flight experiences

● Wind tunnel test - validation/verification

● Change of vehicle OML to reduce ascent acoustics– MPCV experience

● Limitations observed from flight data

Abort Acoustics

● Lack of prior experience and database

● Creation of database from Static Fire test – spectral trends, shock amplitude

● Challenge of simulating hundreds of abort scenario within a reasonable budget
○ Hot helium to simulate rocket plume
- similarity parameters
- scaling problems
○ Increasing Flight Mach shows a reduction in overall levels, but increases low freq content.
○ Plume impingement generally reduces level of pressure fluctuations

● Comparison with flight data from Pad Abort 1:
○ Not an apple-to-apple comparison: different shape, transient flight vs steady simulation
○ Nonetheless, comparable overall level and the spectral shape

● Unique, one-of-a-kind test provides aeroacoustics environment for the design and qualification testing of ORION/MPCV Launch Abort Vehicle which is meant to save astronauts lives.

BACKUP

Summary:

- Unobstructed plume: noise sources are distributed along the plume
- In a launch configuration: locations where plume impinges on solid surfaces are the primary sources
  - ► Current Lift-off models (SP8072) does not account for impingement
    - Need investments in changing/updating these models
  - ►Minimization of plume impingement will attenuate liftoff environment
    - ○ By reduce vehicle drift in early part of liftoff
    - ○ Possibly by increasing the MLP hole size

- Open/Uncovered part of the trench are noise sources
  - ○ Closing the trench as much as possible will reduce liftoff environment

- Water injection in the hole & trench is effective in reducing trench generated noise
- On-Deck water (Rainbird) is partially effective in noise source mitigation

- Microphone phased-array is an ideal tool to study all launch acoustic environments
  - Results from the current study are expected to help SLS pad design

Future work:

Looking for opportunities to use phased-array in full-scale launch

Reference:

1. Himelblau, H., Myron Fuller, C. & Scharton, T. D., “Assessment of Space Vehicle Aeroacoustic-Vibration Prediction, Design and Testing,” *NASA CR-1596,* July 1970.
2. Cockburn, J.A. & Robertson, J. E., “Vibration Response of Spacecraft Shrouds to In-Flight Fluctuating Pressures,” J. Sound & Vib. **33**(4), pp. 399-425, 1974.
3. Hughes, W. O., McNelis, A. M. & Himelblau, H., “Investigation of Acoustic Fields for the Cassini Spacecraft: Reverberant Versus Launch Environments,” AIAA paper 99-1985, 1999.
4. Apollo flight environment data book – ref??
5. Rockwell International and Space Shuttle Vibration and Acoustics Group, “ Space Shuttle System Acoustics and Shock Data Book,” *SD 74-SH-0082B*, June 1987.
6. Jones, G. W., & Foughner, J. T., “Investigation of Buffet Pressures on Models of Large Manned Vehicle Configurations,” NASAS TN D-1633, 1963
7. Hill, R. E., & Coody, M. C., “Vibration and Acoustic Environments for Payload/Cargo Integration,” *AIAA paper 83-0329*, Jan 1983.
8. Dougherty, N.S., & Guest, S. H., “A Correlation of Scale Model and Flight Aeroacoustic Data for the Space Shuttle Vehicle,” AIAA paper 84-2351, Oct 1984.
9. Leger L. J. “Space Shuttle Bay Environment,” AIAA paper 83-2576-CP, 1983.
10. Panda, J., Martin, F. W., Sutliff, D. L., "Estimation of the Unsteady Aerodynamic load on Space Shuttle External Tank Protuberances from a Component Wind Tunnel Test," AIAA paper 2008-0232, presented at AIAA Aerospace Sciences Meeting, 2008.
11. Panda, J., Burnside, N. J., Bauer, S. X. S., Scotti, S. J., Ross, J. C. & Schuster, D. M., 2009 “A comparative Study of External Pressure Fluctuations on Various Configurations of Launch Abort System and Crew Exploration Vehicle” AIAA paper 2009-3322
12. Panda, J., James, G. H., Burnside, N. J., Fong, R. K., Fogt, V. A. & Ross, J. C., “Use of Heated Helium to Measure Surface Pressure Fluctuations on the Launch Abort Vehicle During Abort Motor Firing,” AIAA paper 2011-2901.
13. Panda, J., Mosher, R. N. & Porter, B. J., “Identification of Noise Sources During Rocket Engine Test Firings and a Rocket Launch Using a Microphone Phased Array,” NASA TM-2013-216625, Dec. 2013.
14. Eldred, K. M. & Jones, G. W., Jr., “Acoustic load generated by the propulsion system,” NASA SP-8072, 1971.
15. Brehm, C., Sozer, E., Moini-Yekta, S., Housman, J. A., Barad, M. F., Kiris, C. C., Vu, B. T. & Parlier, C. R., “Computational Prediction of Pressure Environment in the Flame Trench,” AIAA paper no 2013-2538.
16. Panda, J. & Mosher, R., “Microphone Phased Array to Identify Liftoff Noise Sources in Model-Scale Tests,” Journal *of Spacecraft and Rockets*, Vol. 50, No. 5, Sept-Oct 2013. DOI: 10.2514/1.A32433
17. Reed, D. K., Melody, M. N. & Nanace, D. K., “An Assessment of Ares I-X Aeroacoustic Measurements with Comparisons to Pre-Flight Wind Tunnel Test Results,: AIAA paper 2011-174, 2011.
18.

Ascent Acoustics

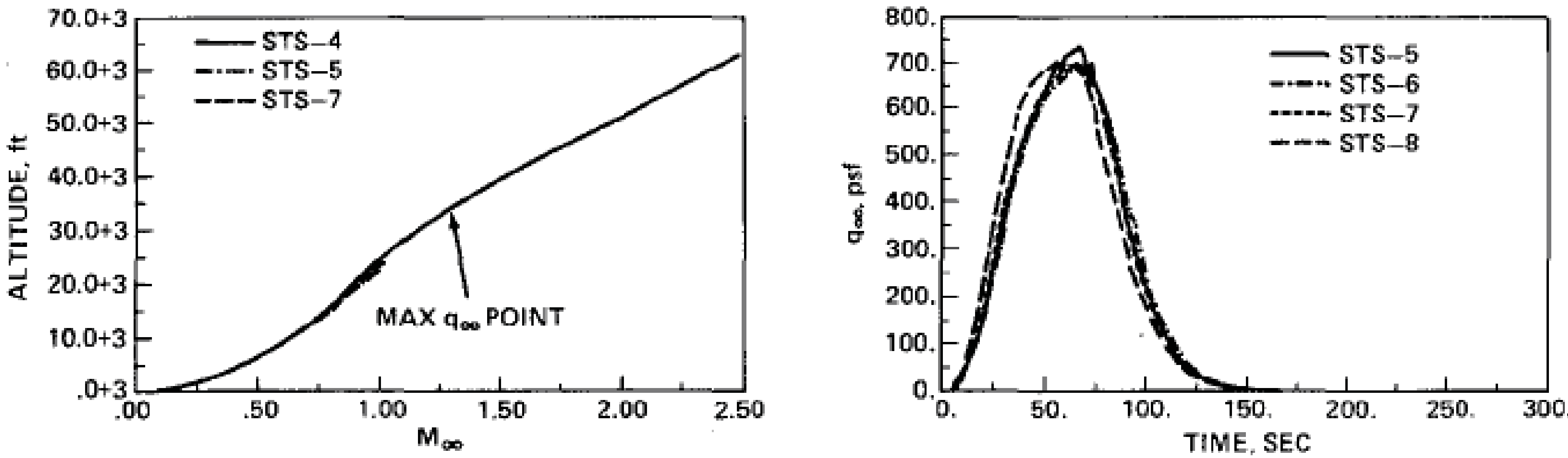

Fig 4 Typical ascent flight trajectories

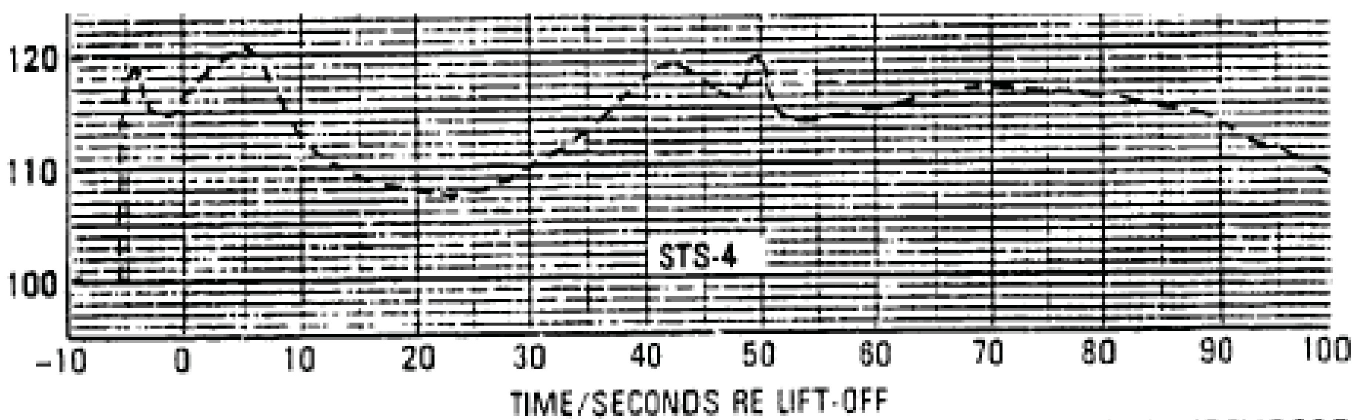

Figure 1.3-2. STS Aero/Acoustic Noise Level Time History – Crew Cabin – Flight Deck

Phased array in Antares Engine Test: Feb 22, 2013

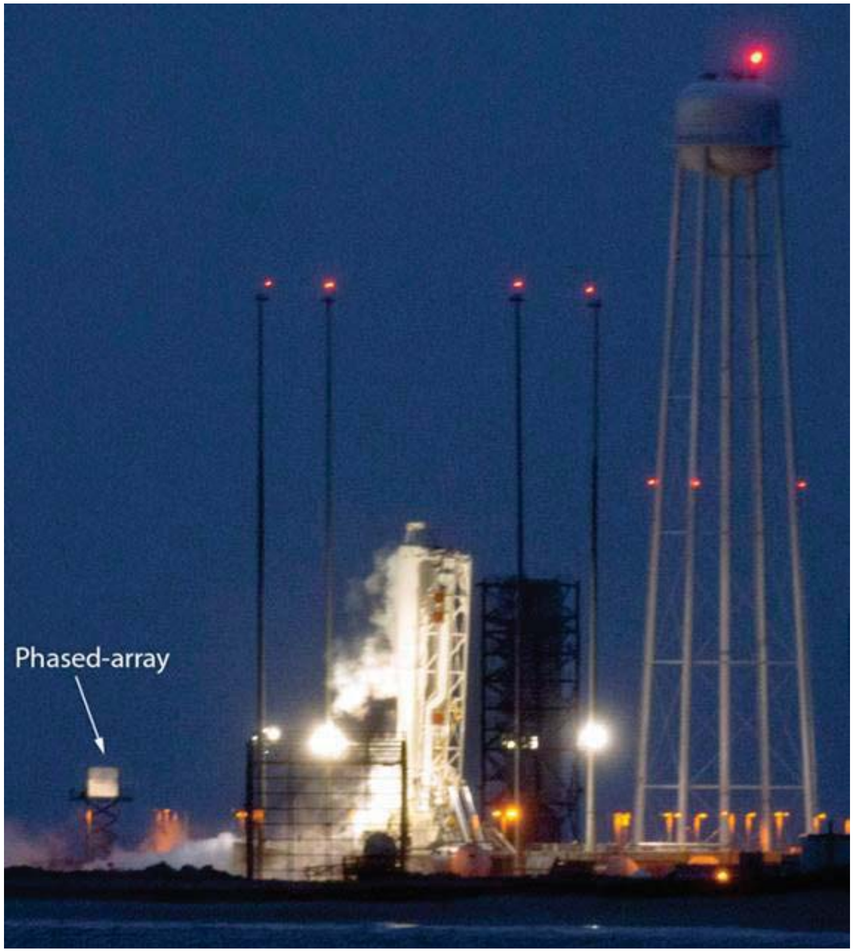

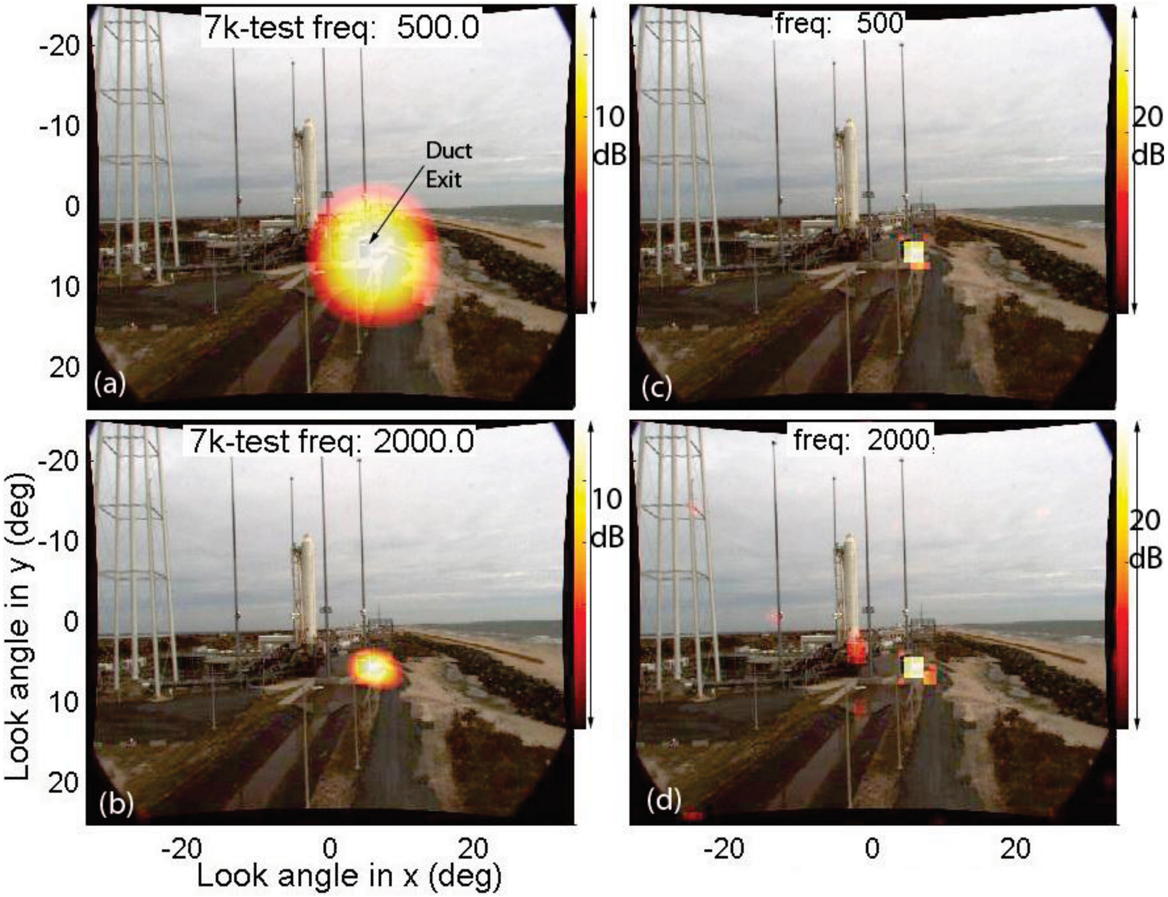

Summary of results from Engine Test:

- The primary noise source was the duct exit
- Plume out of the duct exit was NOT a primary source - very large amount of water pumped at the duct inlet quenched the flame
- Noise generated during impingement on the deflector, and general mixing inside the duct, emerged out of the duct exit.
- First time application of phased array in full-scale engine test